MICROBIAL INFLUENCED CORROSION ON *ACCOMAC*, A FRESHWATER, FERROUS-HULLED SHIPWRECK: EVALUATION OF MICROBIAL DIVERSITY AND COMPOSITION

By

Maggie Shostak

May, 2023

Director of Thesis: Erin K. Field

Major Department: Biology

Abstract

Abandoned shipwrecks are sitting at the bottom of oceans and lakes around the world, deteriorating extensively as the years pass by. Over time, however, microbial-comprised biofilm formation on these structures has resulted in the degradation of these structures and their integrity. The overall structure, abundance, and diversity of microbial communities on shipwrecks have only recently been studied in marine water environments. While previous studies have looked at the microbial communities associated with shallow water wrecks in marine environments, studies focusing on freshwater wreck systems are still unknown. The purpose of this study was to determine microbial community diversity trends and microbial community abundance taxa trends across the Accomac shipwreck. Furthermore, shipwrecks are colonized by corrosion-causing taxa, such as iron-oxidizing bacteria (FeOBs) and sulfate-reducing bacteria (SRBs) which have been shown to influence the biocorrosion of ferrous-hulled structures. Identification of the various microbes in biofilms, as well as corrosion-causing microbes, can help researchers understand the role they play in aquatic ecosystem development and persistence. A total of 44 Biofilm shipwreck samples were collected from various regions across the shipwreck, as well as 5 sediment samples and water samples which were also

collected around the ship. DNA extractions on biofilm samples were conducted and sent for 16S amplicon sequencing to determine full community presence and diversity trends. Results suggest there was a statistically significant difference between the various sample types (i.e., biofilm, sediment, and water), indicating the microenvironments around the Accomac shipwreck influence the composition of the biofilm communities. The primary taxa responsible for significant differences between the microenvironments included *Bacteroidata*, *Chloroflexi*, and Cyanobacteria. Water samples had a higher taxa richness compared to shipwreck biofilm and sediment samples, indicating the mixing of water due to current movements aids in biofilm diversity and microbial community composition. Microbial diversity was not affected by the distinct side of the wreck (i.e., port side vs starboard side), and each had a similar community makeup. This suggests that the increase wave action on the port side of the wreck didn't influence community composition. Water depth was a statistically significant factor influencing the clustering of amplicon sequence variants (ASVs) at the different sample locations (i.e., waterline, below waterline). This suggests that greater depths influence the taxonomic makeup of biofilm communities. Overall, the results from this study showed similar trends in microbial community assemblages which were influenced by the microenvironment they were found in, shallow wrecks are similar to those seen in marine systems indicating similar microbes play a role in biofilm formation.

MICROBIAL INFLUENCED CORROSION ON *ACCOMAC*, A FRESHWATER, FERROUS-HULLED SHIPWRECK: EVALUATION OF MICROBIAL DIVERSITY AND COMPOSITION

A Thesis

Presented to the Faculty of the Department of Biology

East Carolina University

In Partial Fulfillment of the Requirements for the Degree

Master of Science in Biology

By

Maggie Shostak

May, 2023

Director of Thesis: Erin Field, Ph.D.
Thesis Committee Members:
April Blakeslee, Ph.D.
Ariane Peralta, Ph.D.
Nathan Richards, Ph.D.

ACKNOWLEDGEMENTS

I would like to thank my thesis advisor, Dr. Erin Field, and committee members, Dr. April Blakeslee, Dr. Ariane Peralta, and Dr. Nathan Richards, for their support, guidance, and contributions to my thesis work. Specifically, thank you to Dr. Erin Field for her guidance in the development of my project and research questions, as well as Dr. Nathan Richards for his expertise in underwater maritime archeology. I would also like to thank Allyson Ropp and the Maritime Archaeology field school for assistance in sample collection. Special thanks to my undergraduate research assistant, Meredith Cox, for her help in sampling collection and laboratory analyses as I could not complete it without her. I am grateful to the American Museum of Natural History (AMNH) for providing funding for this project through their Theodore Roosevelt Memorial Fund. I would also like to thank Dr. Susan Langley and the Maryland Historical Trust for permission to obtain non-invasive hull scrapings on *Accomac* to study the microbial community trends (*Sampling Permit #202201*). I would also like to thank Dr. Michael Brewer and Cody Garrison for their assistance and proficiency in RStudio pipeline techniques. Finally, I want to thank my parents, James, and Susan Shostak. They have supported me throughout both my undergraduate and graduate career; I would not be where I am today without you!

TABLE OF CONTENTS

LIST OF TABLES

LIST OF FIGURES

LIST OF SYMBOLS OR ABBREVIATIONS

CHAPTER 1 – OVERVIEW OF LITERATURE

INTRODUCTION

Throughout history, iron and steel-hulled ships have sailed across Earth's oceans transporting people and various goods; however, many either sink to the bottom of a river, ocean, and/or lake, or are decommissioned (*Hampel et al., 2022*). In time, they take on a new role in the environment as artificial reefs (ARs) for the vast community of organisms who claim freshwater and marine water as their home (*Hamdan et al., 2021*). They also serve as a historical 'stamp' in time, but due to natural chemical and biological processes the iron and steel-hulled shipwrecks eventually corrode, leading to deterioration and loss of integrity of the wreck (***Fig. 1***). This is caused by the microbially-influenced corrosion (MIC) communities of sulfate-reducing bacteria (SRB) and iron-oxidizing bacteria (FeOB) feeding on the byproducts of the degradation of those components (*Enning et al., 2014*). Visual confirmation of MIC can include "rusticles", discolorations of the metal, or the presence of slimes/sludges. The type of metal substrates can influence the assemblage of microbes established on ARs (*White et al., 1990*).

Iron is one of the most abundant resources on earth, especially within Earth's crust, meaning it has become a key energy source for many microbes (*Henri et al., 2016*). Stainless steel is used in a variety of industries such as infrastructure, mechanics, or home improvement as it is greatly resistant to corrosion in a multitude of environments (*Moreno et al., 2014*). Iron and steel are not only major components of modern-day shipbuilding but are also the key constructional material for infrastructure, such as oil and gas pipelines (*Beech et al., 2005*). The degradation of these structures underwater has resulted in billions of dollars being spent on maintenance, repairs, and replacement (*Vigneron et al., 2018*). In literature, corrosion can be measured as total structure or physical loss in either millimeters (mm) or micrometers (μm) to

help estimate, and in some cases predict, the rate of long-term reliability of infrastructure (*Melchers, 2014*). The study of iron-oxidizing microbes has become more popular in the scientific community as they are one of the major players in biocorrosion which impact overall gross domestic product (GPD) across the world (*Dobretsov et al., 2019*; *Emerson, 2019*). Iron-oxidizers are separated into group based on how they can oxidize iron: (i) aerobically, (ii) neutrophilically, (iii) anaerobically, or (iv) photosynthetically (*Hedrich et al., 2011*). FeOB can also be separated into different classes of *Proteobacteria* depending on their environments; marine FeOB belongs to the class *Zetaproteobacteria* while freshwater FeOB belongs to the *Betaproteobacteria* (*McBeth et al., 2013*). To distinguish which environmental water is considered marine or fresh, the salinities in parts per thousand (ppt) must fall within a certain range. Marine water salinity measurements average 35 ppt, whereas freshwater salinities measure 0.5 ppt or lower (*Vinogradova et al., 2019*). Furthermore, salinity has become a major factor in the determination of microbial communities, especially those communities in seawater (*De França et al., 2000*). Salinization of freshwater systems has also become an increasing issue due to climate change as this has impacted various ecosystems (*Vineis et al., 2011*).

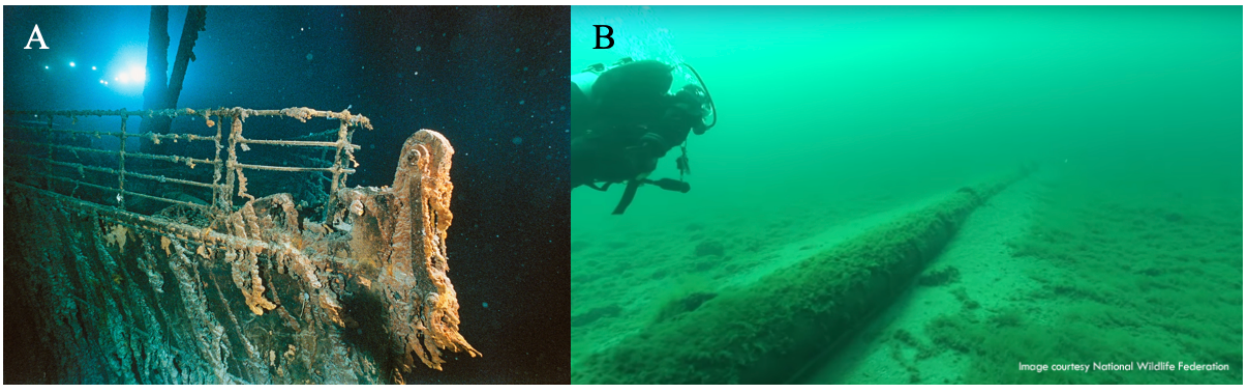

Figure 1. (A) Rusticles present on RMS Titanic due to microbially influenced corrosion (MIC) as it sits on the bottom of the Atlantic Ocean. (B) Underwater pipelines are prone to corrosion and can result in oil spills, gas spills if they break. [Figure adapted from (A) *Emory Kristof, National Geographic* and (B) *Line 5 oil pipeline in Straits of Mackinac*, *National Wildlife Federation*]

Two mechanisms have been determined to play an important part in microbially influenced corrosion: (1) electrical microbiological influenced corrosion (EMIC), also known as type I corrosion, and (2) chemical microbiologically influenced corrosion (CMIC), also known as type II corrosion (*Xu et al., 2014; Xu et al., 2017*). Type I corrosion (EMIC) occurs as electrons from steel or iron are oxidized and then immediately uptaken by the microorganisms; however, the corrosion byproducts produced through EMIC depend on the ionic environment (*Telegdi et al., 2017*). Type II corrosion, on the other hand, (CMIC) occurs when the iron reacts with hydrogen sulfide and other corrosive compounds, as well as other fermentative or sulfidogenic bacteria (*Venzlaff et al., 2013*).

Environmental Influences on Biofilm Formation and Artificial Reefs

Biofilms, first discovered by Antonie van Leeuwenhoek as he observed tooth surfaces under a microscope, are defined as an assembly of different microbial organisms attached to a surface structure forming an enclosing extracellular polysaccharide matrix (*Donlan, 2002*). Diversity is considerably high as bacteria, archaea, fungi, protozoa, and viruses can all be components of the biofilm matrix (*Besemer, 2015*). The formation of them on these structures further promotes corrosion, due to the establishment of the perfect ecological niche for the microbial communities (*Dubiel et al., 2002*). Other factors influencing biofilm formation include interspecies interactions and the resiliency of the biofilm (*Mugge et al., 2019*). Extreme weather events due to climate change, such as rising temperatures and excess flooding, results in an increase of nutrients in water systems. This results in greater nutrient availability for biofilms, leading to higher growth rates and increased promotion of microbially influenced corrosion (*Usher et al., 2014*).

Current Research on Shipwreck Biofilm Communities

Research on shipwreck biofilm communities, including corrosion-causing microbes, is a relatively new field of interest, with most research focusing on deep-water marine environments (*Hamdan et al., 2018; Johnson et al., 2006; Marsili et al., 2018*). Research on 19th-century World War II shipwrecks in the Gulf of Mexico shows that microbial communities have an "island effect" when proximal to shipwrecks (*Hamden et al., 2018*).

A research team from East Carolina University traveled to Rodanthe, NC to survey the microbial communities responsible for the corrosion of a marine water shipwreck, Pappy Lane (*Price et al., 2020*). This ferrous-hulled wreck, based on circumstantial evidence is most likely a landing craft support vessel [LCS(L)(3)] from the World War II era within the Pamlico Sound of North Carolina. The salinity of the Pamlico Sound ranges anywhere from 17.0 parts per thousand (ppt) to 27.0 ppt, with seasonal, tidal, and wind influences. The drilled ship cores and visibly corroded debris samples were analyzed to determine the relative abundance of iron-oxidizing bacteria (FeOB), as well as community analysis, through DNA extractions via a Qiagen DNeasy PowerSoil Kit, quantitative PCR, and culturing of FeOB species on Modified Wolfe's Mineral Medium (MWMM freshwater medium) used for the cultivation of FeOB from freshwater environments. Findings by Price suggest niche partitioning by different taxa influences microbial community composition. In other words, the microbial community structure depends on where they are found (on the shipwreck, in the sediment, or the water). Furthermore, niche partitioning also influenced taxa differences in visibly corroded sections of the wreck compared to non-visible corroded sections. *Zetaproteobacteria* were found to have a higher relative abundance in visibly corroded sections of the wreck, compared to non-visible corroded sections of the wreck. The taxa that were found to lead to significant differences between community composition

between sediment samples and shipwreck samples included the classes *Alphaproteobacteria*, *Deltaproteobacteria*, and *Gammaproteobacteria*. Similar trends were seen on the most probable number (MPN) plates, with higher relative abundance on plates containing visible corrosion.

Little is known about biofilm formation in freshwater, shallow shipwrecks, or if taxonomic trends follow those found in marine systems (*Garrison et al., 2021*). Studies by Besemer et al. (*2022*) show that freshwater biofilms are primarily comprised of *Proteobacteria*, *Bacteroidetes*, and *Cyanobacteria*. Furthermore, research has been conducted on microbially influenced corrosion of steel and iron structures located in freshwater environments. Peng et al suggest that surrounding environmental factors can influence microbial community composition, as well as the relative abundance of corrosion-causing taxa. Research of a shallow, freshwater wreck in Mallows Bay, Maryland will aid in filling in some of these knowledge gaps about freshwater biofilm communities, as well as corrosion-causing microbes on ferrous-hulled structures.

Historical Importance

Historically, Captain John Smith explored and documented the Potomac River, as well as the shoreline known today as Mallows Bay. Mallows Bay was once a remote and insignificant inlet; however, it eventually became the final resting place of hundreds of ships utilized during the 20th century. Currently, these wrecks have been dubbed the "Ghost Fleet of Mallows Bay" (***Fig. 2***). During the summer season, large concentrations of green algae (*Chlorophyta*) and blue-green algae (*Cyanophyta*) are present, although their concentrations are gradually decreasing due to the introduction of an invasive species of water thyme (*Hydrilla*). During the winter season, the abundance of freshwater diatoms, such as *Bacillariophyta*, and green algae *Chlorophyta* are

significantly less. The flora and fauna located within this region have become unstable due to the introduction of these ships and salvaging efforts resulting in the use of explosives and excavation (*Shomette, 1998*).

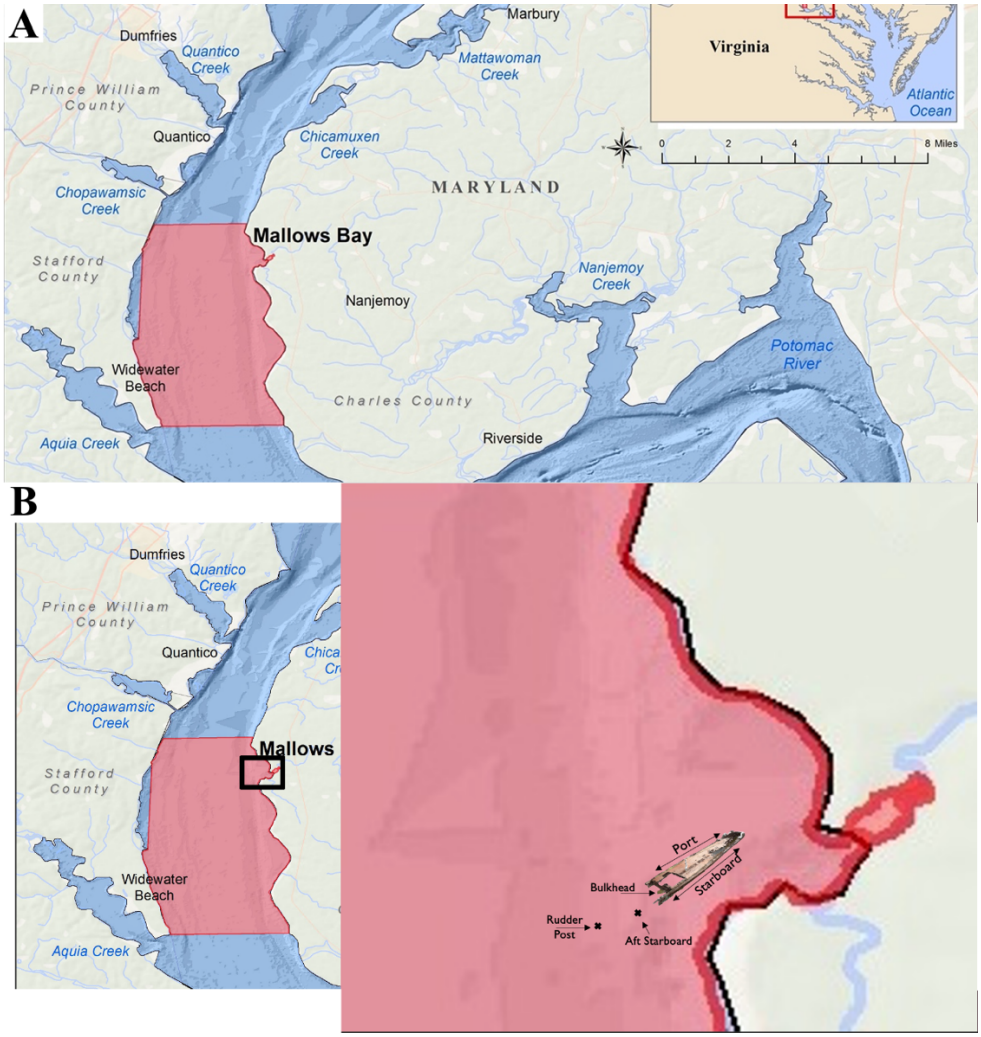

Figure 2. (A) Map showing the location of Mallows Bay (in red) of the Potomac River in Charles County, Maryland. (B) Orientation of Accomac wreck in Mallows Bay with biofilm sampling locations labeled. [Figure adapted from (A) *NOAA NGDC*, *GEBCO*, *Esri*, *De Lorme*, and *other contributors* and (B) *Black box and transposed Accomac figure Shostak, M additions*]

In 1917, President Woodrow Wilson called for the United States to take up arms against Germany, officially entering our nation into World War I (WWI). Expecting the war to last over several years, American shipbuilders constructed and launched 192 ships in 1916. Through the

establishment of the Emergency Fleet Corporation (EFC), over 1,000 wooden steamships were planned for construction as well as other various types of ships such as barges and steel-hulled vessels. Unfortunately, timber supply issues, delivery timing, and labor shortages resulted in delays to the program, leading to little satisfaction with shipping board officials. Although many ships were successfully launched and utilized during WWI, many were left inactive in ports once our nation entered the era of the Great Depression (*Shomette, 1998*).

In April of 1920, a committee appointed by Admiral Benson and Eugene Meyer Jr was established to move and dispose of unwanted wooden steamships. The fleet of ships was initially towed and dismantled off the shores of Widewater, Virginia; however, due to backlash and complaints from both local fisherman and government officials, roughly 200 ships eventually were hauled into Mallows Bay, Maryland by September of 1925 (***Fig. 3***).

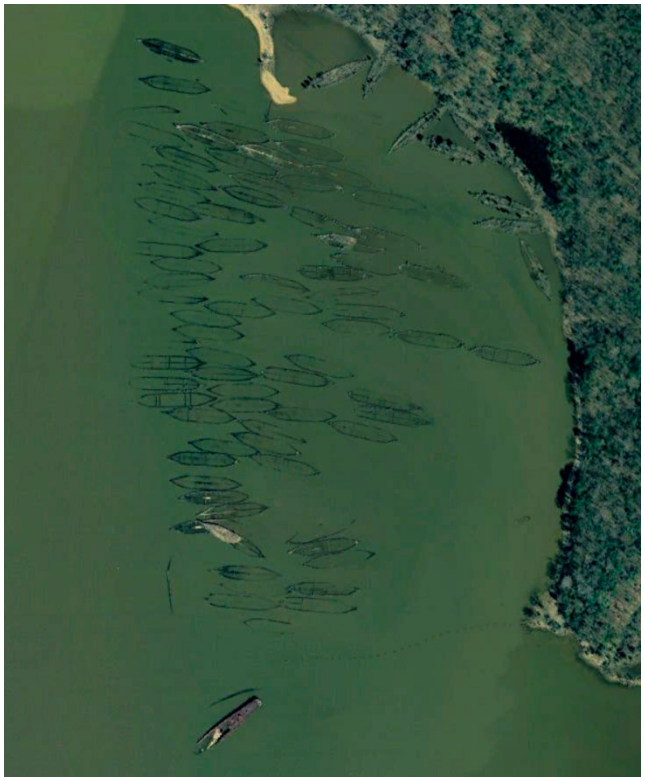

Figure 3. Overhead view of the "Ghost Fleet" of Mallows Bay in Charles County, Maryland. [Photo sourced from *Google Earth*]

Once there, many of the ships were burned, and their hulls beached. Charles County residents salvaged the burned and sunken steel hulls of the ships to used and sold for scrap metal, with an official decree set in place on January 15, 1936. The start of the United States participation into World War II, began with the Japanese attack on the United States Pacific Fleet at Pearl Harbor, Hawaii, in 1941. The U.S. government then sponsored a salvaging project on the ship lying in Mallows Bay (*Shomette, 1998*).

The only steel-hulled vessel located in Mallows Bay is *Accomac*, ex-*Virginia Lee* (***Fig. 4***). *Virginia Lee* was originally built for the Pennsylvania Railroad (PRR) in 1928 in Quincy, Massachusetts. During WWII, I was requisitioned by the US Government and was placed in service to transport rubber on the Amazon River in Brazil. By 1952, *Virginia Lee* was converted into a car ferry for the Virginia Ferry Corporation where it shuttled cars between Boston, Plymouth, and Province. Unfortunately, it caught fire in 1964 and was removed from the car ferrying service. By 1973, Accomac was hulled into Mallows Bay (*Shomette, 1998*). Research on this shallow, freshwater wreck will aid in filling in some of these knowledge gaps about freshwater biofilm communities, as well as the taxa responsible for freshwater microbial influenced corrosion.

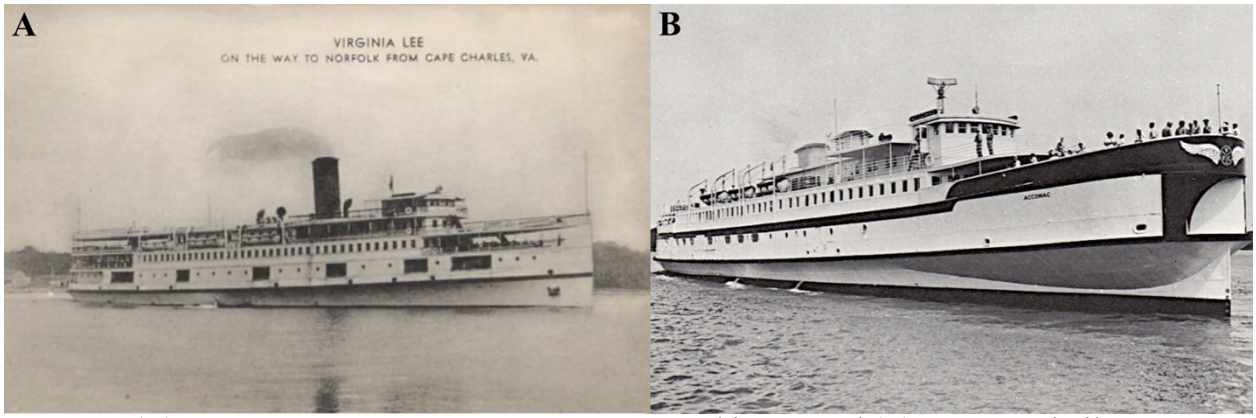

Figure 4. (A) Steamer Ex-*Virginia Lee*, c1928 post card image and (B) Accomac built as Virginia Lee repurposed as a car ferry. [Photos sourced from (A) *Cape Charles Historical Society*, *Cape Charles*, *VA* and (B) *Mariner's Museum*, *Newport News*, *VA*]

CHAPTER 2 – DISTINCT MICROBIAL COMMUNITY ABUNDANCE AND DIVERSITY TRENDS ACROSS *ACCOMAC*

This study aims to determine the relative species abundance and community diversity trends across a freshwater shipwreck (*Accomac*) located in Mallows Bay, Charles County, Maryland (***Fig. 5***). Understanding microbial community patterns across the wreck can help researchers determine how microbes assemble on wrecks and within the wreck environments. Additionally, identification of the iron-oxidizing and sulfate-reducing bacteria in these communities will help determine which species may play a role in the biocorrosion of ferrous-hulled structures. Most organisms, whether they are microbes, plants, or animals, have certain requirements (resources) for them to survive and replicate. These requirements collectively referred to as an ecological niche, can distinguish which types of organisms are present. Through the integration of microbial community data, and understanding, plus the creation of predictive models, management strategies can be developed and implemented to preserve not only *Accomac*, but also other ferrous-composed structures across the globe.

Figure 5. Present day *Accomac* shipwreck hull, located in Mallows Bay, Maryland. [Photo sourced from *Amaury Laporte*]

RESEARCH QUESTION AND HYPOTHESES

Community Diversity & Relative Species Abundance

Does microbial community composition differ based on the microenvironment? Are there differences in microbial community abundance between the Starboard side versus the Port side of the freshwater shipwreck, *Accomac*? I hypothesized that microbial community composition would be different in the various microenvironments as each act as its own environmental niche.

Is depth a significant factor for microbial community abundance and species diversity? I hypothesized that biofilm samples collected at the water line would have more microbial community diversity compared to samples below the waterline. This is due to the increased wave action seen on the port side of the wreck, which would lead to more environmental resilience by the microbes.

MATERIALS AND METHODS

Field Sampling

The only ferrous-hulled shipwreck, *Accomac*, is in the Mallows Bay Marine Sanctuary (*National Oceanic and Atmospheric Administration, NOAA*) at 38°28'08.0" N, 77°16'10.9" W. The wreck is 88.7m long (291.1ft) and its orientation is southwest-to-northeast with the bow of the ship facing northeast, bearing 46º. The stern has been dismantled and much of the ship has been gutted by scrappers (***Fig. 6)*** The ferrous hull remains flat and is anchored by stone, with shellfish and subaquatic vegetation in the flooded hold of the ship. Salinity measurements of the freshwater system ranged from 0.3-1.9ppt, with low wind speeds and mild wave movement. Moderate wakes occurred occasionally due to recreational boats passing by at roughly 150m away from the wreck. Biofilm samples were collected at 0m, 1.5m, 2.5m 27.5m, 28m, 28.5m,

53.5m, 54.5m, 55.5m, and 78.1m across the wreck (***Fig. 7, Fig. 8***). Specific sampling locations included the after-quarters, the bulkhead, the rudder post, the port (left) side, and starboard (right) side. Three replicate samples were collected at each of those locations at distinct water depths: waterline and below the water line (***Fig. 9 – Fig. 12***).

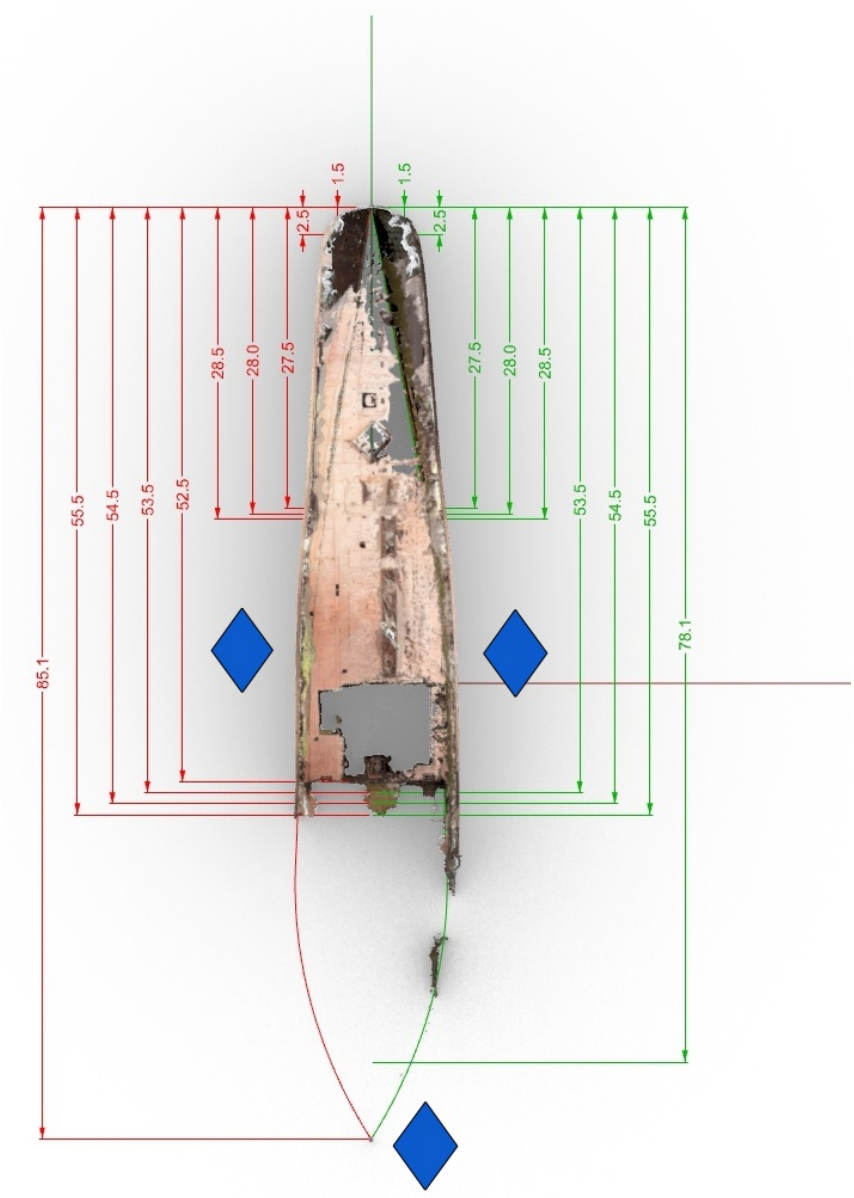

Figure 6. Isometric 3D top-view model (*RhinoCAD-derived*) of Accomac shipwreck sampling distances (in meters) on both port side (red) and starboard side (green). Blue diamond's representing water samples taken on port side, starboard side and by the rudder post.

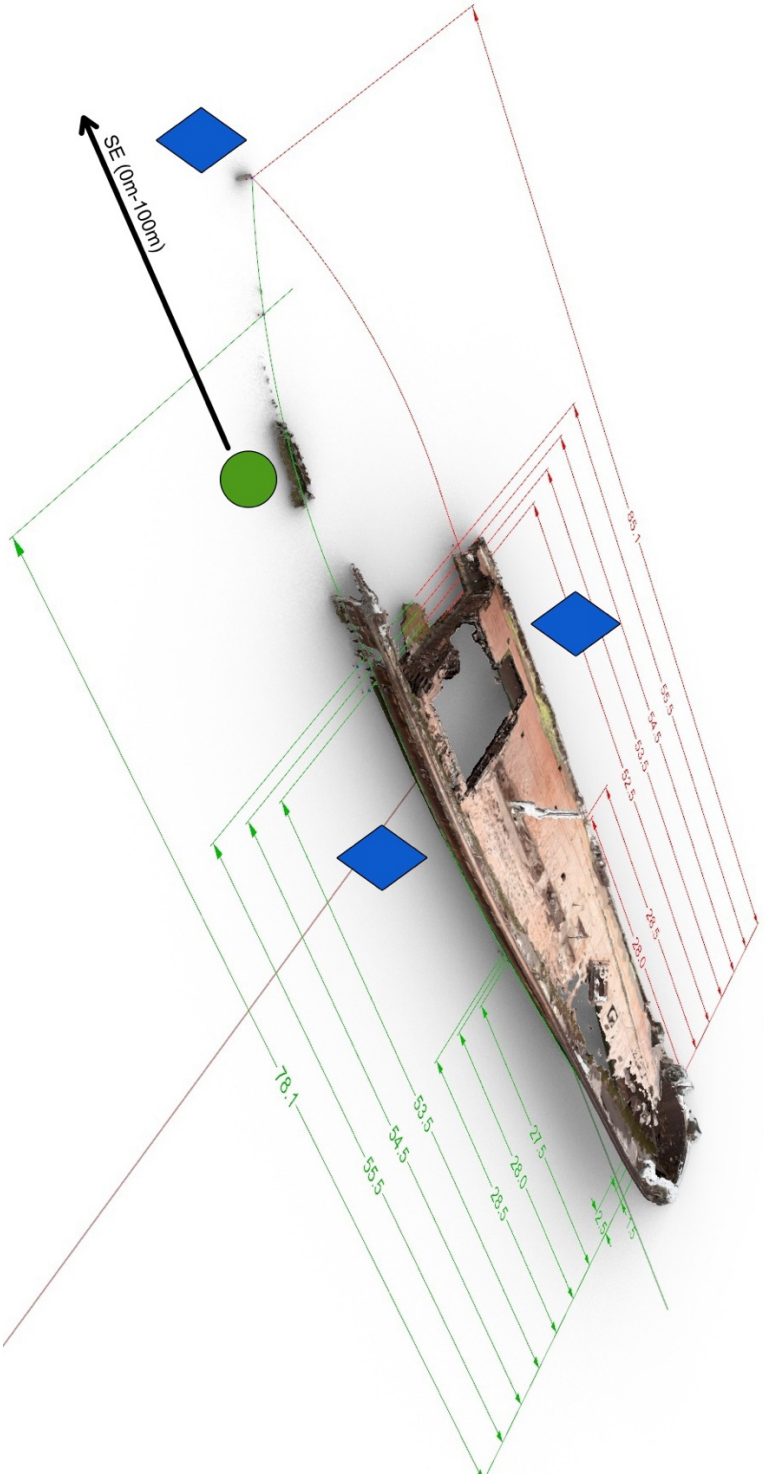

Figure 7. Isometric 3D top-view model (*RhinoCAD-derived*) of Accomac shipwreck sampling distances (in meters) on both port side (red) and starboard side (green). Blue diamond's representing water samples taken on port side, starboard side and by the rudder post. Green circle represents 25m increment (0m to 100m) sediment transect bearing SE.

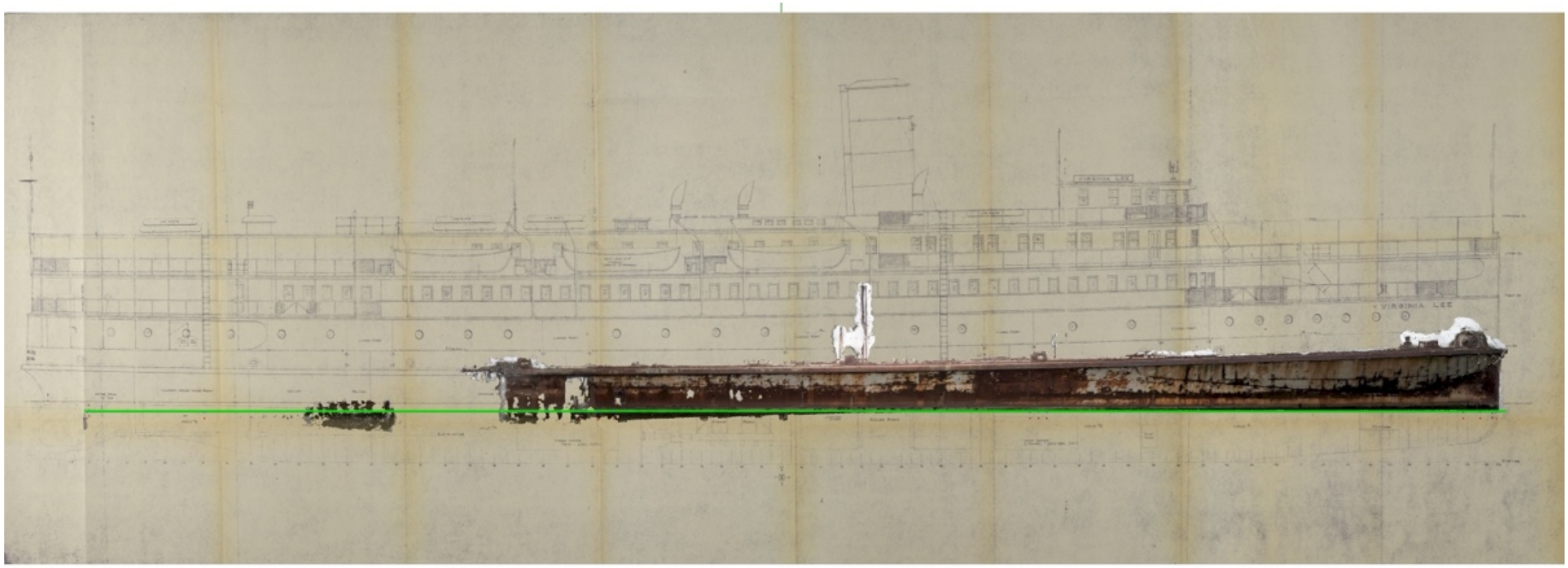

Figure 8. 3D model (*RhinoCAD-derived*) of the remaining hull (starboard view) of *Accomac* shipwreck overlayed onto original blueprints. Green line represents water line level.

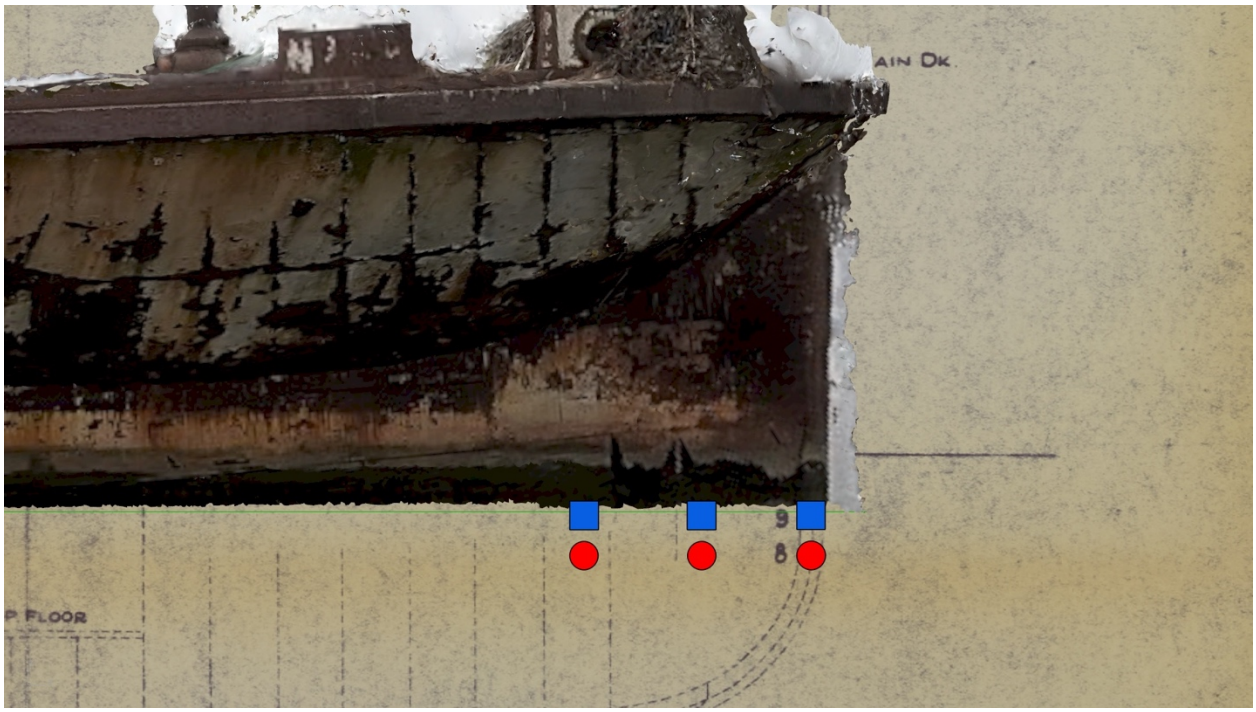

Figure 9. 3D model (*RhinoCAD-derived*) of starboard side (right) *Accomac* shipwreck overlayed onto blueprints showing bow (front) biofilm samples. Blue squares represent biofilm samples taken at the water line and red circle samples represents biofilm samples taken below the waterline.

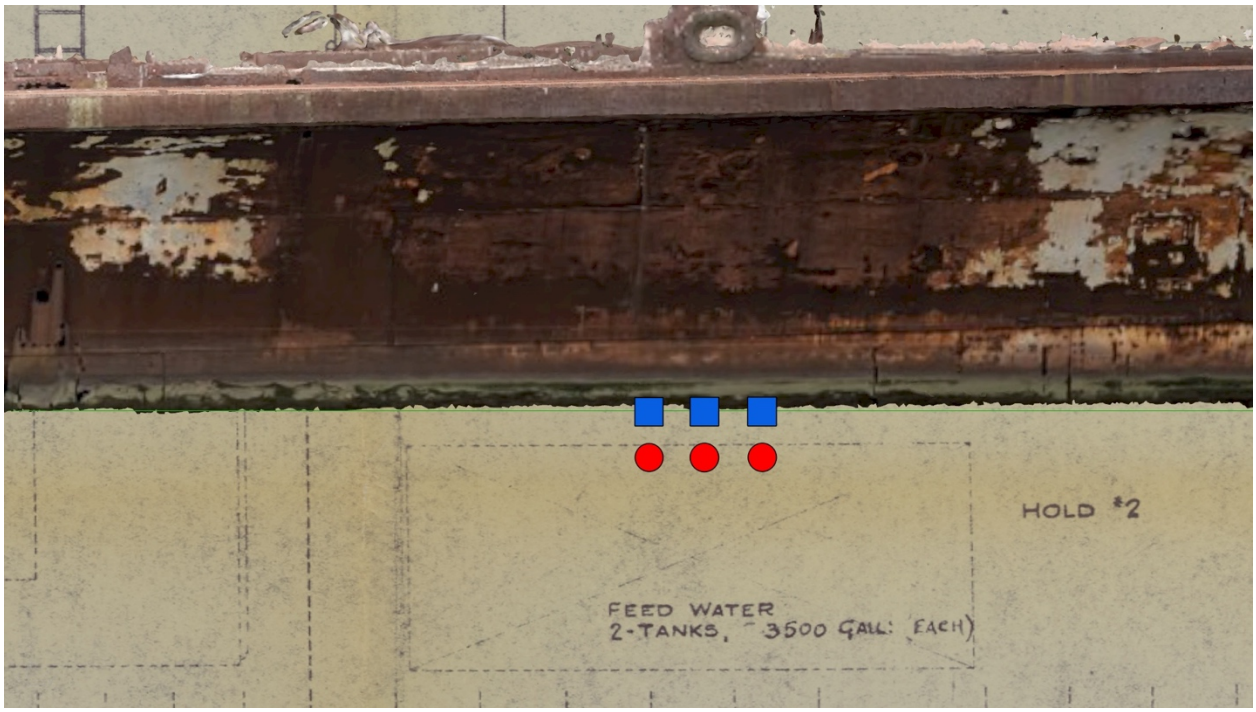

Figure 10. 3D model (*RhinoCAD-derived*) of starboard side (right) *Accomac* shipwreck overlayed onto blueprints showing middle (front) biofilm samples. Blue squares represent biofilm samples taken at the water line and red circle samples represents biofilm samples taken below the waterline.

Figure 11. 3D model (*RhinoCAD-derived*) of starboard side (right) *Accomac* shipwreck overlayed onto blueprints showing bulkhead (back) biofilm samples. Blue squares represent biofilm samples taken at the water line and red circle samples represents biofilm samples taken below the waterline.

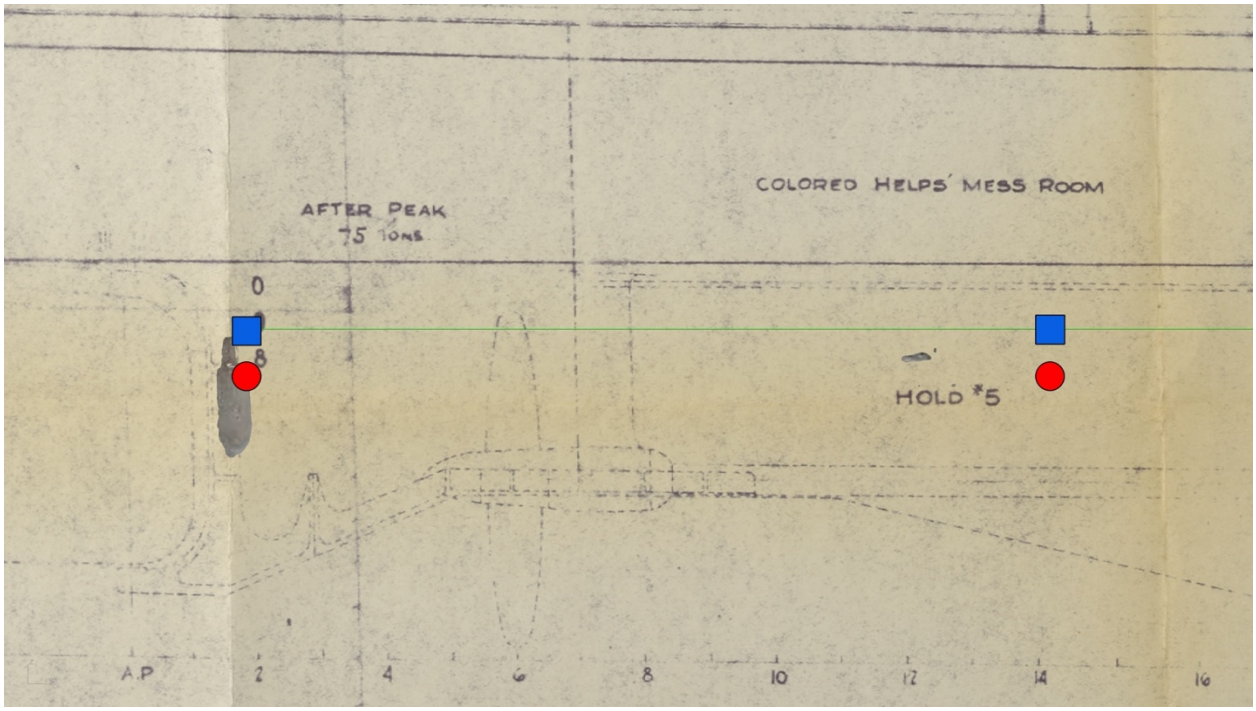

Figure 12. 3D model (*RhinoCAD-derived*) of starboard side (right) *Accomac* shipwreck overlayed onto blueprints showing the rudder post (grey) biofilm samples and after-quarter (submerged under water) biofilm samples. Blue squares represent biofilm samples taken at the water line and red circle samples represents biofilm samples taken below the waterline.

Polypropylene scrapers were used to prevent any damage to the wreck and 50mL conical tubes were used to collect biofilm samples. Five sediment samples were collected in 25m increments (0m-100m) in a southwest transect, starting at the after-quarters. Three water samples were collected on the port side, starboard side and rudder post locations filling a 2000 mL plastic container. All samples were placed in a cooler filled with ice packs and transported back to the laboratory located at East Carolina University, Greenville, North Carolina for further processing (***Table 1***, ***Table 2***).

Table 1. Shipwreck biofilm samples across various locations, distances, and water depths

PORT SIDE					STARBOARD SIDE				
# Samples	**Distance (across wreck)**	**Location**	**Depth**	**Water Level**	**# Samples**	**Distance (across wreck)**	**Location**	**Depth**	**Water Level**
3	0m 1.5m 2.5m	Bow	0ft	Waterline	3	0m 1.5m 2.5m	Bow	0ft	Waterline
3	0m 1.5m 2.5m	Bow	0.3ft	Below Waterline	3	0m 1.5m 2.5m	Bow	0.3ft	Below Waterline
3	27.5m 28m 28.5m	Middle	0ft	Waterline	3	27.5m 28m 28.5m	Middle	0ft	Waterline
3	27.5m 28m 28.5m	Middle	0.3ft	Below Waterline	3	27.5m 28m 28.5m	Middle	0.3ft	Below Waterline
3	53.5m 54.5m 55.5m	Stern	0ft	Waterline	3	53.5m 54.5m 55.5m	Stern	0ft	Waterline
3	53.5m 54.5m 55.5m	Stern	0.3ft	Below Waterline	3	53.5m 54.5m 55.5m	Stern	0.3ft	Below Waterline

RUDDER POST			BULKHEAD		
# Samples	**Depth**	**Water Level**	**# Samples**	**Depth**	**Water Level**
1	0ft	Waterline	1	0ft	Waterline
1	0.3ft	Below Waterline	2	0.3ft	Below Waterline

Table 2. Shipwreck biofilm samples from the exposed portion of the starboard side after-quarters, water samples and sediment samples. Sediment sample 0m was collected at the rudder post and then collected in 25m increments in a southwest transect.

AFT STARBOARD				WATER SAMPLES	
# Samples	Depth	Water Level	Distance (across wreck)	# Samples	Location
3	3ft	Below Waterline	78.1m	10	Port Side
				10	Starboard
				3	Rudder Post

SEDIMENT		
# Samples	Distance	Depth
1	0m	5ft
1	25m	5ft
1	50m	5ft
1	75m	5ft
1	100m	5ft

DNA Extraction

Water sampled from each of the three sample locations around *Accomac* were filtered through 25 µm paper disc filters at 500 mL increments, ten times for a total of 30 filtration discs for each DNA extraction. A DNeasy PowerSoil Pro kit (Qiagen Inc.) was used to extract DNA from both the water filter discs and the shipwreck samples, as it provided the best quantity of DNA when used in previous studies (*Garrison et al., 2019*; *Price et al., 2020*). The PowerBead Pro tubes were centrifuged briefly to ensure all the beads are settled at the bottom of the container and then weighed before the samples are added. Scrapings from the sampling locations were added to each properly labeled PowerBead Pro tube and weighed again to determine the final mass. After all the tubes are filled with samples, 800µL of Solution CD1 was added to each tube and then vortexed briefly. Samples were homogenized (higher DNA yields) by placing the tubes on a vortex adaptor horizontally at a maximum speed of 10 minutes. PowerBead Pro tubes will then be centrifuged for 1 minute at 15,000 x g and the resulting supernatant (roughly 600µL) was transferred to a clean 2mL microcentrifuge tube. 200µL of Solution CD2 is added to each

tube, then vortexed briefly, before samples were centrifuged again at 15,000 x g for 1 minute. Avoiding the pellet, 700µL of supernatant was transferred to a clean 2mL microcentrifuge tube and then 600µL of Solution CD3 was added, vortexing each briefly. 650µL of the lysate was transferred into MB Spin Columns containing filtered membranes and then centrifuged again at 15,000 x g for 1 minute. Flow-through was discarded and the rest of the lysate was added to the MB Spin Column to ensure all DNA has bonded to the filter membrane. After the resulting flow-through was discarded, the MB Spin Column was placed in a clean 2mL collection tube and 500µL of Solution EA (wash buffer) was added to remove proteins and other non-aqueous contaminants from the filter membrane. The tube was once again centrifuged at 15,000 x g for one minute and the resulting flow-through was discarded. The MB spin column was placed back into the same 2mL collection tube before 500µL of Solution C5 was added to further clean the DNA that was bound to the silica filter membrane in the spin column. The tube was centrifuged at 15,000 x g for one minute and flow-through was discarded before placing the MB spin column in a clean 1.5mL elution tube. The elution tube was centrifuged for 2 minutes at 16,000 x g to remove residual Solution C5 so the ethanol would not interfere with downstream DNA applications. After centrifuging, 60µL of Solution C6 was added to the center of the white filter membrane, to result in a more efficient and complete release of DNA from the filter, before centrifuging the tube once more at 15,000 x g for 1 minute. The MB spin column was ultimately discarded, and the DNA was stored in a -80°C freezer until it was ready to be used for downstream applications.

Quality Control

The Qubit 2.0 fluorometric system (Invitrogen) is a fluorescence-based device used to determine the quantity of double-stranded DNA (ng/µL) extracted from each sample (*Nakayama et al. 2016*). A Nanodrop spectrophotometer was used to analyze the quantity of total extracted DNA (ng/µL) as well as reporting the protein purity ratio (A260/A280, optimal DNA value 1.8) and the salt purity ratio (A260/A230, optimal DNA value over 2.0). The resulting absorbance spectrum graph indicates if there are any contaminants in the sample before sending it off to a sequencing laboratory (*Brock, 2019*). Both Qubit and Nanodrop are recommended devices for quality checks as only a small amount of DNA needs to be placed in the device and has an array of uses for different downstream applications; next-generation sequencing, genotyping, and qRT-PCR. Integrated Microbiome Resource laboratory services were used for amplicon sequencing via Illumina MiSeq and require a minimum of 1ng/µL, although a higher preference for more than 10 ng/µL, of concentrated DNA in each submitted sample. IMR prefers A260/230 ratio above 2.0 and needs a total volume of 10µL for each sample submitted. An estimated amplicon read length of 1,000 is needed as it was sequenced using Illumina's 300+300 bp pair-ended chemistry.

Library Preparation and Amplicon Sequencing

Next-generation sequencing (NGS) has become the most popular platform for various sequencing technology companies due to higher throughputs, lower error rates, and a reduction in prices (*Kchouk et al., 2017*). Specifically, Illumina MiSeq was chosen due to achieving the highest throughput with long reads when it was compared to other NGS platforms such as Ion Torrent or 454 Roche (*Loman et al., 2012*). DNA was extracted from the iron debris samples

using a QIAGEN PowerSoil DNA kit and then the library will then be prepped using KAPA Hyper Plus. After library preparation, samples were plated on a 96-well plate (20µL of sample per well) and then sent to the Integrated Microbiome Resource (IMR) at the Centre for Comparative Genomics and Evolutionary Bioinformatics at Dalhousie University in Nova Scotia, Canada for 16S rRNA bacterial amplicon sequencing. The fragments were amplified by PCR by utilizing Illumina adaptors and recommended IMR V6-V8 primer targets. This region was specifically chosen as studies have shown it to have better coverage of short bacterial sequences, compared to the commonly used V4-V5 primer target regions (*Comeau et al., 2011*; *Swanson, 2020*). The samples were then run on an Illumina MiSeq machine using 300+300 bp paired-end V3-chemistry following protocols described in (*Comeau et al., 2017*).

Data Analysis

Sequences were subsequently loaded into R statistical environment as demultiplexed fastq files and run through the dada2 pipeline R package (*R Development Core Team, 2017*). DADA2 utilizes an algorithm that results in the procurement of high-resolution amplicon sequence variant (ASV) tables instead of the traditional operating taxonomic unit (OTU) table (*Callahan et al., 2016*). ASVs have become an alternative method for microorganism clustering as they maintain broad-scale ecological patterns and can provide better insight into "fine-scale" patterns otherwise masked (*Callahan et al., 2017*; *Glassman and Martiny, 2018*). Paired reads were trimmed at 280bp and 200bp for forward and reverse sequences, respectively to remove any bases with a low average quality score. A maxEE=c(2,2) was used so a maximum of 2 ambiguous nucleotides in a row for both the forward and reverse reads before there are tossed out of the algorithm. Dereplication (i.e., removal of sequences that are 100% identical) was

performed to remove any redundant sequences and to reduce total computational time. Sequences were then merged, those that didn't were removed, and any chimeric sequences were removed. Chimeric sequences are defined as those that can be produced by stitching two abundant sequences. Taxonomy was then assigned to all remaining sequence variants. Vegan and ggplot packages via tidyverse were utilized to create taxonomic stacked bar charts at various taxonomic levels to represent community composition for the different sampling groups (*Wickham, 2017*). Non-metric multidimensional scaling (NMDS) plots were constructed using the R package vegan and ggplot2, with a set seed of 1000 (*McMurdie and Holmes, 2013*; *Wickham, 2016*). Differences between sample location, specific sides of the wreck, and water depth were calculated using a Bray-Curtis index from the resulting ASV counts, rarefaction of the alpha diversity indices is still in the process of computation (*Morris et al., 2014*). The produced matrix was then used to calculate the Shannon's H diversity, the taxa richness and the Pielou's evenness indices (*Oksanen et al., 2017*). A simper analysis was run to calculate the contribution of each taxon (%) to the dissimilarity between the different biofilm sampling group locations. Specifically, which taxonomic groups, if any, were significantly contributing to the dissimilarity between microbial community composition (*Khomich et al., 2021).* Significant ASVs and their corresponding taxonomic classification from the simper analysis were separated out from the rest of the data to visualize the taxa significant for these differences at various levels (i.e., classes, orders, or families). Beta-diversity measurements were completed through the use of an analysis of similarity (ANOSIM) test and a Permutational multivariate analysis of variance (PERMANOVA) test. An analysis of similarities (ANOSIM) was run to compare the means of ranked dissimilarities between sampling groups to the mean of ranked dissimilarities within sampling groups, although it has been found to be sensitive to heterogeneity (*Anderson and*

Walsh, 2013).. The statistic R determines the measure of similarity of mean ranks between and within the sampling groups. The p-value evaluates the significant differences between two or more groups. The PERMANOVA tested the centroids, which are similar to means, for each group to determine significant differences.

RESULTS AND DISCUSSION

Comparison of Bacterial Composition of Shipwreck Site

To determine any dissimilarity, or similarity, between the microbial communities based on sampling location, an NMDS analysis was performed with a stress value of 0.08. There was a statistically significant difference between the sampling locations and the microbial community composition was dissimilar between the different samples' locations (*ANOSIM*: *R=0.4937; p=0.001*). Shipwreck biofilm samples clustered together with the exception of biofilm samples taken on an exposed section of the after-quarters which suggests the microbial communities were distinct at the after-quarters compared to the rest of the shipwreck biofilm communities. (***Fig 13. Points A-D***). A potential explanation for this distinction could be that the after-quarter samples were taken at greater depth (3ft) compared to the other biofilm samples. This could influence the formation of the biofilm communities as well as the community composition. Alternatively, the microenvironment varied more greatly in comparison to the other shipwreck microenvironment which lead to the distinct cluster of the ASVs. Water samples clustered together which suggests microbial communities are similar in composition regardless of whether water was sampled on the starboard side, port side, or by the rudder post. Sediment microbial communities were more similar to each other, but showed more variability in their composition as they were not clustered as tightly as the other sample types. Community dissimilarities among sediment samples suggest

the individual sediment microenvironments are more heterogeneous as you increase distance away from the wreck. For example, sediment collected 75m away from the wreck did not cluster with other sediment samples (***Fig. 13. Point E***), suggesting that particular microenvironments is different from sediment collected only 25m away from the wreck. Samples were then grouped based on their specific type (i.e., shipwreck biofilm, sediment, or water) and an NMDS analysis with a stress value of 0.07 was used. Similar community clustering was seen as when biofilm samples were separated by their specific locations (***Fig. 14***). These trends suggest a microenvironmental niche partitioning which may be influencing biofilm community composition across the wreck. This is supported by research conducted on an estuarine shallow-water shipwreck similar trends were found by Price et al., 2020.

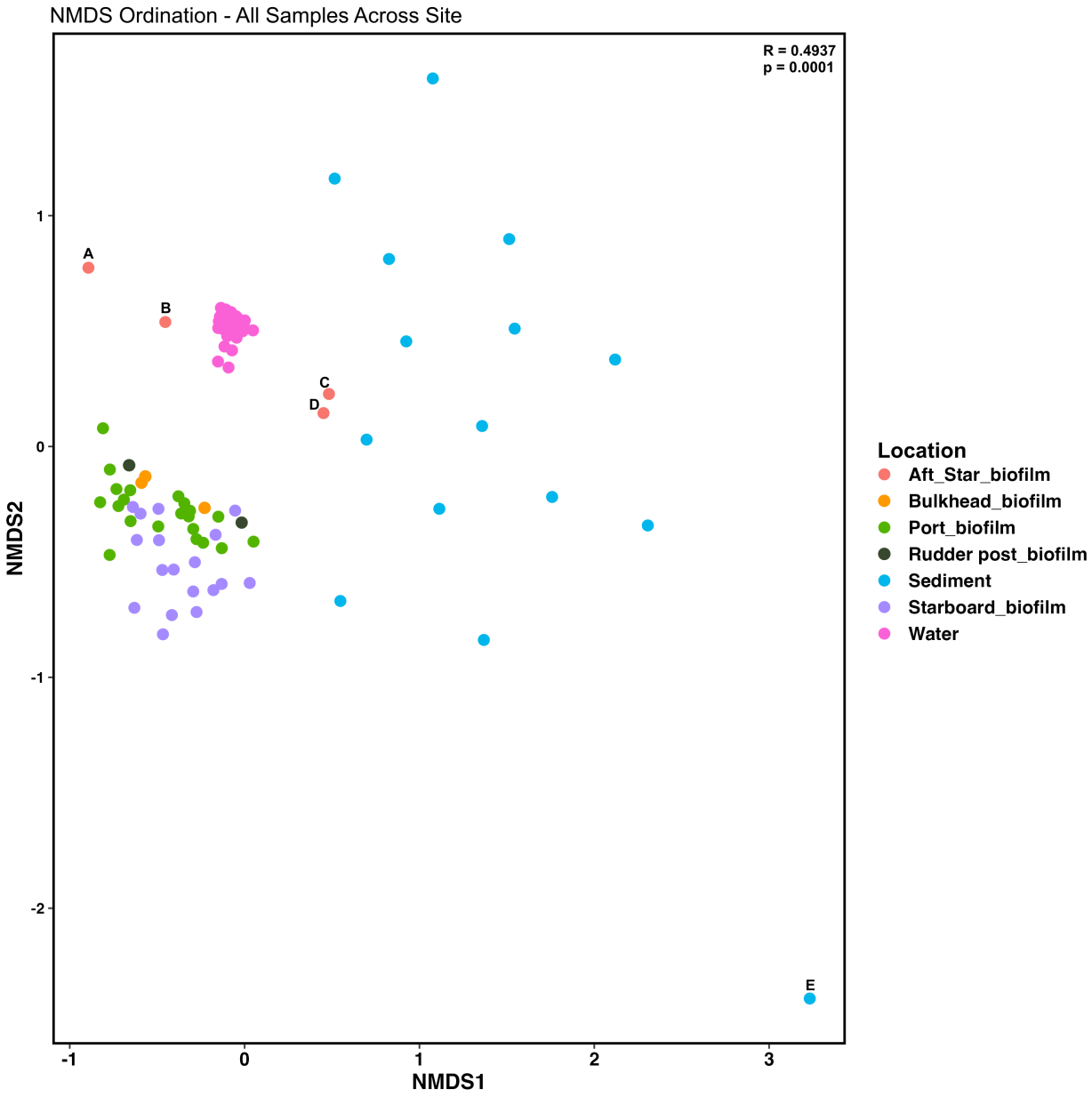

Figure 13. Non-metrical multidimensional ordination plot of the different microenvironmental samples on and around the shipwreck *Accomac*. The microbial community composition is similar between the groups and there was a statistically significant difference between the sampling locations (ANOSIM: $R = 0.4937$, $p < 0.05$). Stress value was 0.08.

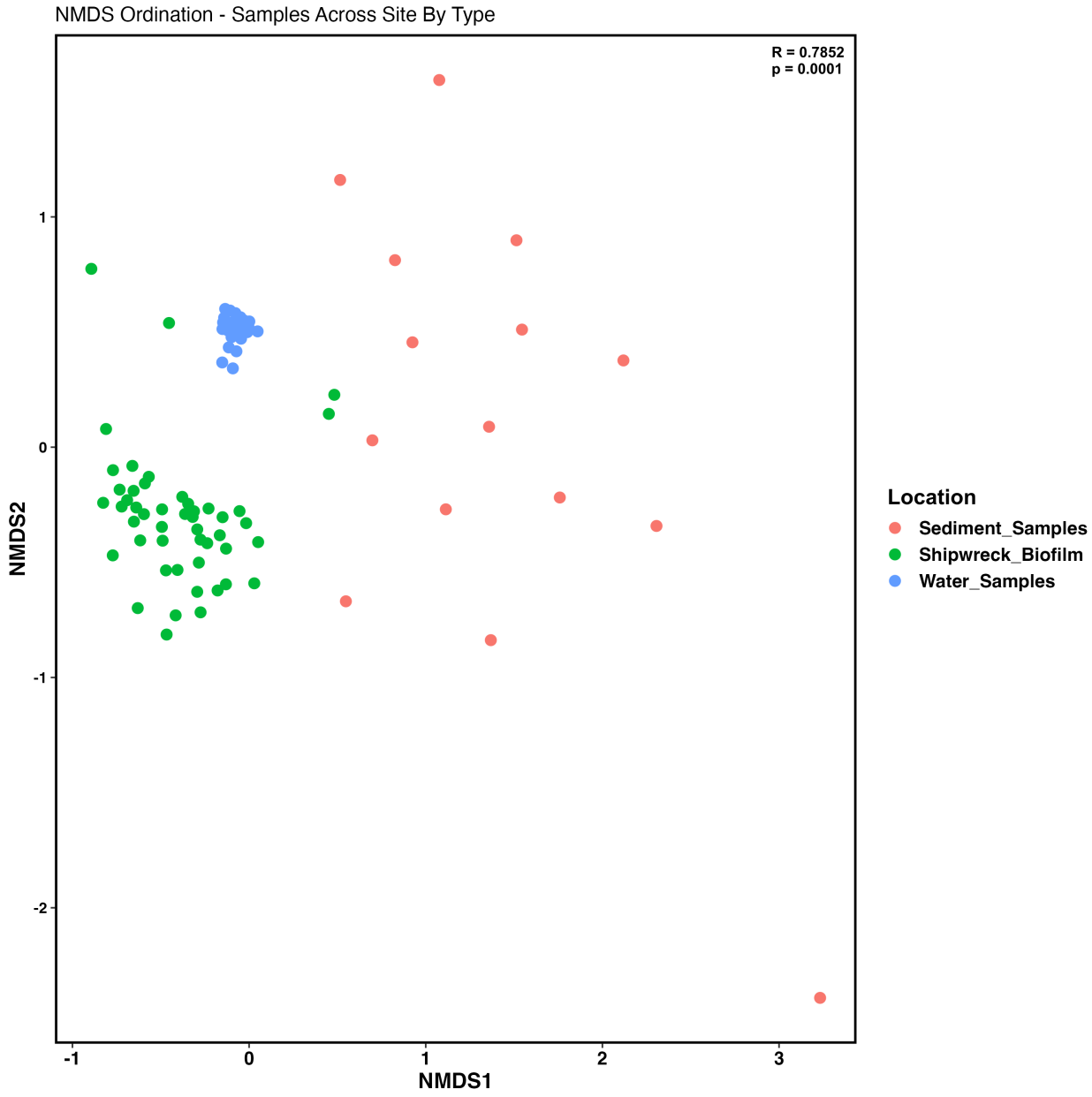

Figure 14. Non-metrical multidimensional ordination plot of the different microenvironmental samples grouped by sample type. Outliers are the same as those noted in *Figure 13*. There was a statistically significant difference between the sediment samples, shipwreck samples and water samples (ANOSIM: $R = 0.7852$, $p < 0.05$). Stress value was 0.07.

To visualize at the taxonomic makeup of the samples across the site, stacked barcharts were created and filtered by the phyla. Taxonomic makeup varied across the wreck with similar relative abundances of certain phyla. For example, the phylum *Acidobacteriota* and *Proteobacteria* showed similar mean relative abundance within shipwreck biofilm samples, whereas the phyla *Nitrospirota* had higher relative abundance in sediment samples (***Fig. 15***). These differences in relative abundances could be influenced by the microenvironments from where the samples were collected from. Dada2 analysis shows that sediment samples had a higher abundance of *MBNT15* compared to surrounding shipwreck biofilm samples and water samples (***Fig. 15***). The bacteria *MBNT15* (GenBank FJ 538146), originally sequenced from rice paddy soil samples in 2009 has been detected in various environments such as soils, marine and freshwater environments, and sediments. Genome analysis conducted by Begmatov et al. reveals specific genes responsible for Fe(III) reduction are encoded by the bacteria. It is also shown to have a close phylogenetic relationship with *Deltaproteobacteria*, which is a known phylum responsible for sulfate reduction (*Quast et al., 2013)*. The high relative abundances of *Proteobacteria* (24.4%) within all samples can be explained by the presence of corrosion causing classes: *Betaproteobacteria* (1.41%) and *Gammaproteobacteria* (52.4%). *Alphaproteobacteria* make up 45.9% of the *Proteobacteria* phylum and are comprised of known phototrophic genera, as described by *Martijn et al., and* the remaining 0.3% of proteobacteria are unclassified. The phylum *Acidobacteriota* makes up of 5.1% of the taxa for all samples, with the majority falling under the class *Vicinamibacteria* (27.9%), *Blastocatellia* (17.7%), and *Acidobacteriae* (15.6%). They have been found in a wide range of habitats around the world, with a majority being identified soil systems (*Kielak et al., 2016*).

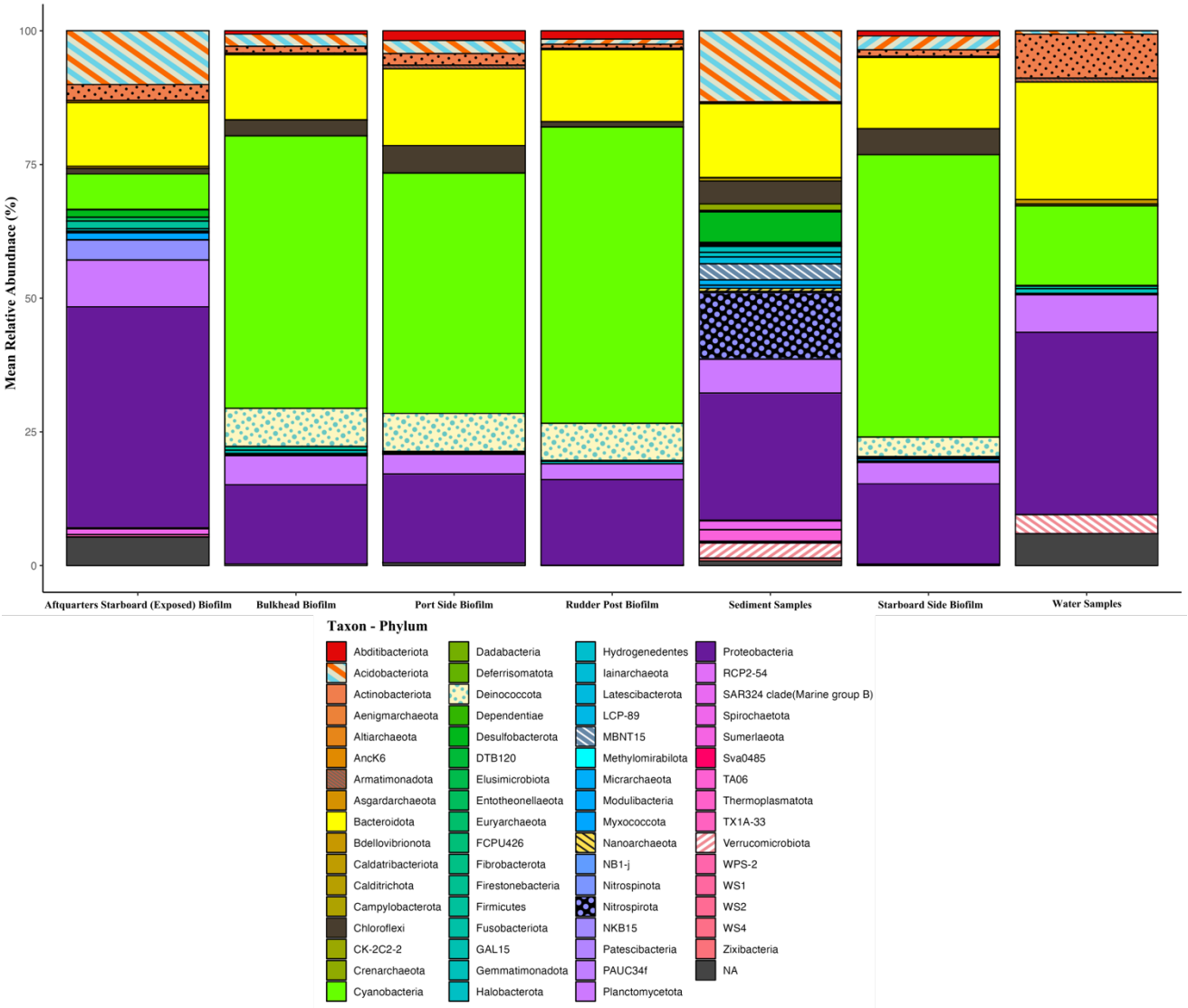

Figure 15. Phylum-level taxonomy barchart based on 16S rRNA gene sequencing data. Water samples, sediment samples and the exposed after quarters on the starboard side had the greatest microbial phylogenetic differences. *Bacteroidata*, *Chloroflexi* and *Cyanobacteria* comprise most of the abundances for shipwreck biofilm samples.

To identify the taxa responsible for the differences observed between the microenvironments, SIMPER analysis was conducted. *Bacteroidata* (60.4%), *Chloroflexi* (23.0%), and *Cyanobacteria* (16.6%) were the primary taxa responsible for significant differences between the microenvironments of the sample locations. The most prevent orders of the *Bacteroidata* phylum from the biofilm samples includes the *Chitinophagales* (27.8%),

Cytophagales (23.9%), *Sphingobacteriales* (13.1%) and *Flavobacteriales* (11.7%) (***Fig. 16***). The most prevalent families included *Chitinophagaceae* (20.2%), *Unclassified Bacteroidetes* (9.47%), and *BSV26* (8.2%) of the *Kryptonailes* order (8.5%) (***Fig. 17***). *Bacteroidetes* are anaerobic, chemo-organotrophs which means they gain energy from organic compounds using chemical energy, gaining electrons from organic compounds such as sugars, fats, and proteins (*Hahnke et al., 2016*). The anaerobic nature of these bacteria supports the large percentage of this specific phylum classified from samples taken at 3ft on the after quarters section where biofilms have less access to oxygen. The second most prevalent phyla, the *Chloroflexi*, were mainly comprised of the orders *Anaerolineales* (29.7%), *Chloroflexales* (12.3%), and *SBR1031* (11.42%) (***Fig. 16***). Most of the families were classified under *Anaerolineaceae* (29.7%), *Unclassified* (28.3%), and *A4b* (8.9%) (***Fig. 17***). The phylum *Chloroflexi* were originally described from samples collected from Crater Lake (Crater Lake National Park, Oregon) and were shown to abundant in freshwater hypolimnion – the lower layer of water – of lakes (*Mehrshad et al., 2018*). Finally, the last most abundant phyla were *Cyanobacteria*, and they were mostly comprised of the orders *Cyanobacteriia* (95.9%), followed by *Sericytochromatia* (2.5%), *Vamprirvibrionia* (1.4%), and *Unclassified* (0.18%) (***Fig. 16***). They are known photosynthetic organisms and have been found in a diverse range of aquatic and terrestrial ecosystems (*Mazard et al., 2016*). Interestingly, the order *Synechococcales* had a higher relative abundance in biofilms sampled from the exposed after-quarters section of the wreck. These orders are important for photosynthetic picoplankton in our global ocean systems and freshwater systems (*Kim et al., 2018*). They have been found to have a reliable adaptation mechanism for changes to different environmental factors such as salinity or light (*Blumwald et al., 1984*). Furthermore, their adaptivity could explain their major prevalence in the after-quarters sample,

which has less light exposure compared to other biofilm locations. This microenvironment could be an established niche for these specific cyanobacteria, due to potentially less competition for resources from other cyanobacteria that cannot thrive in that specific type of environment.

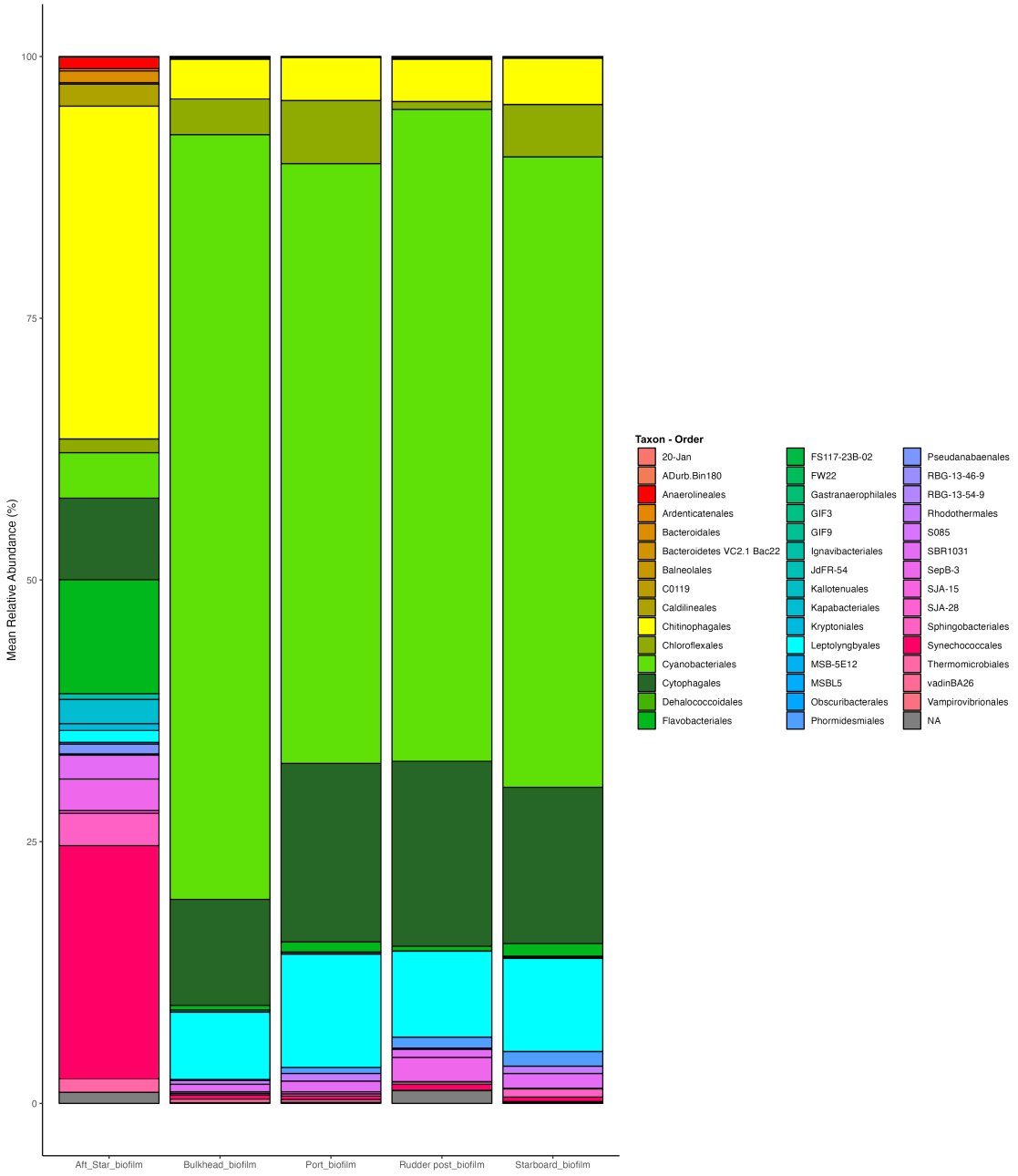

Figure 16. Order-level taxonomy barchart based on Simper significant taxa from original 16S rRNA gene sequencing data. Mean relative abundance calculated only on identified simper significant ASV and doesn't represent abundance for entire biofilm community.

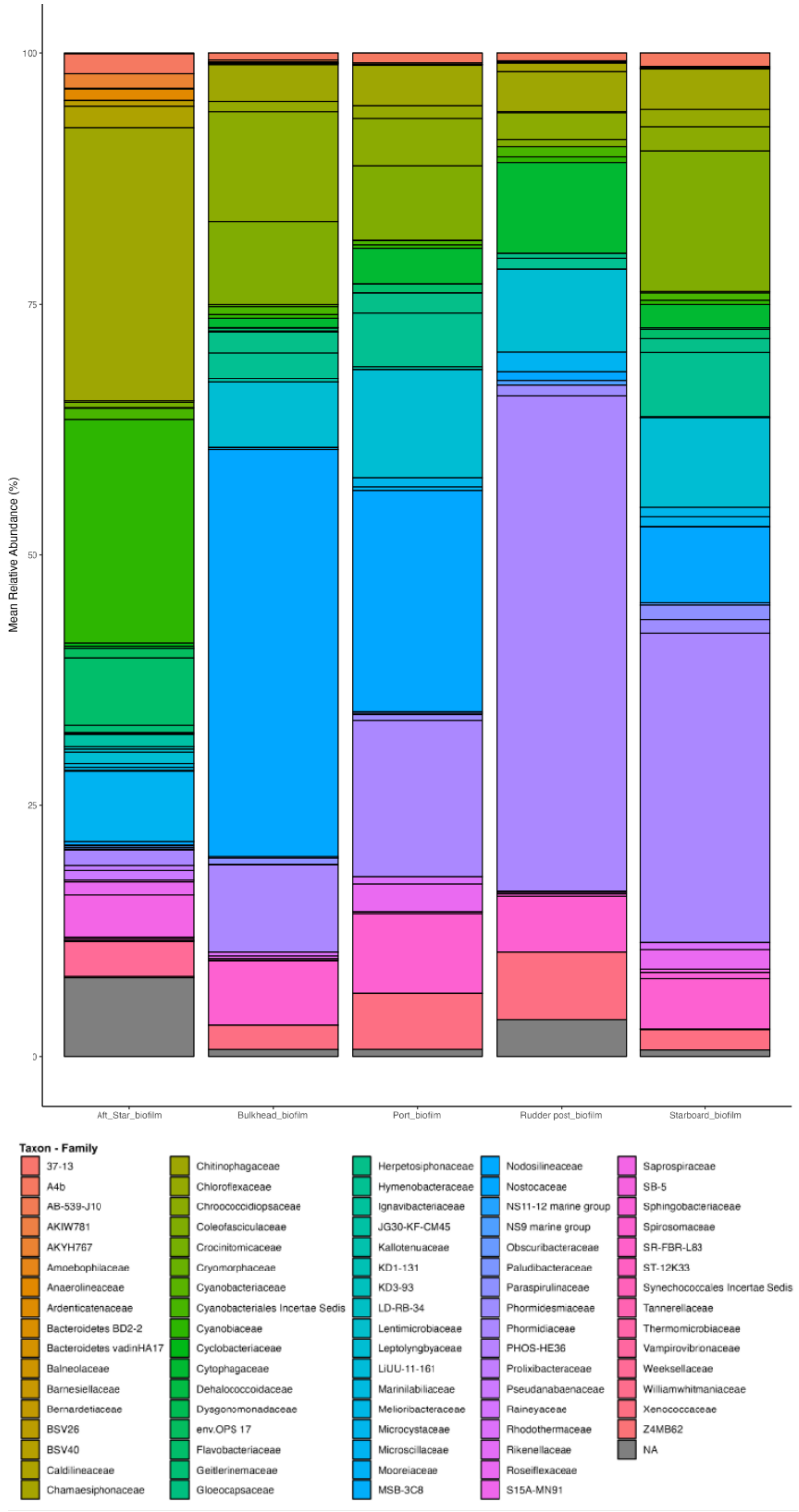

Figure 17. Family-level taxonomy barchart based on Simper significant taxa from original 16S rRNA gene sequencing data. Mean relative abundance calculated only on identified simper significant ASV and doesn't represent abundance for entire biofilm community.

Interestingly, sediment samples were more variable in community composition compared to the other sample types suggesting the sediment niche partitioning applies to a larger variety of taxa. To gain a better idea of which taxa are responsible for microbial community variation within these sediment samples, separate barcharts displaying phyla and class were created. Despite the sediment samples being collected at various distances away from the wreck, the relative abundances of various phyla did not differ between samples (***Fig. 18***) When breaking down the samples into their separate classes, there was still a similar taxonomic makeup between biofilm communities regardless of distance away from the wreck (**Fig. 19**).

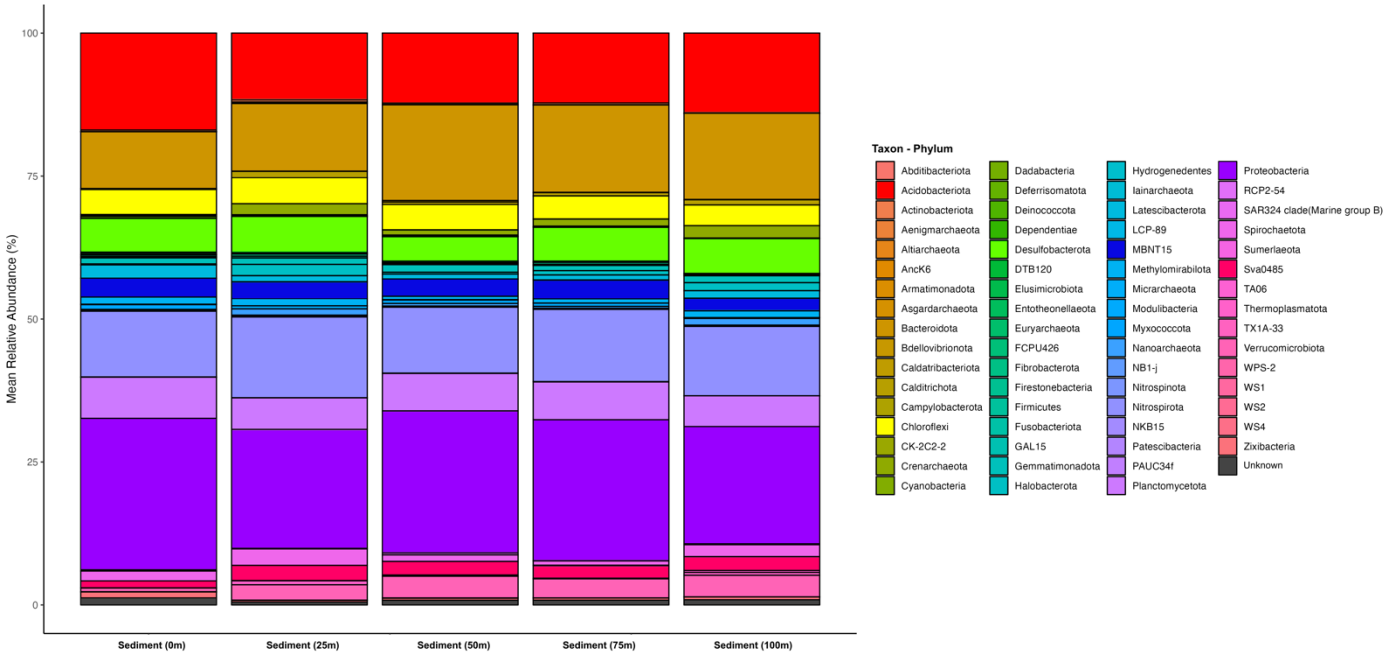

Figure 18. Phylum-level taxonomy barchart based on 16S rRNA gene sequencing data. Sediment samples showed to have similar mean relative abundances regardless of distance from wreck.

To determine if there was any significant difference between sediment samples based on distance away from the wreck, and ANOSIM test was run and an NMDS ordination plot was created. There is no statistically significant difference between sediment samples taken directly

next to the wreck compared to sediment samples taken all the way to 100m away from the wreck (*ANOSIM*: *R=0.0934*; *p=0.2213*; ***Fig. 20***). This suggests the microenvironments of the sediment samples are similar and the presence of the wreck doesn't affect biofilm community makeup. The low R-value corroborates the similar taxonomic makeup between the different sediment samples, as it suggests the microbial community members are similar in composition.

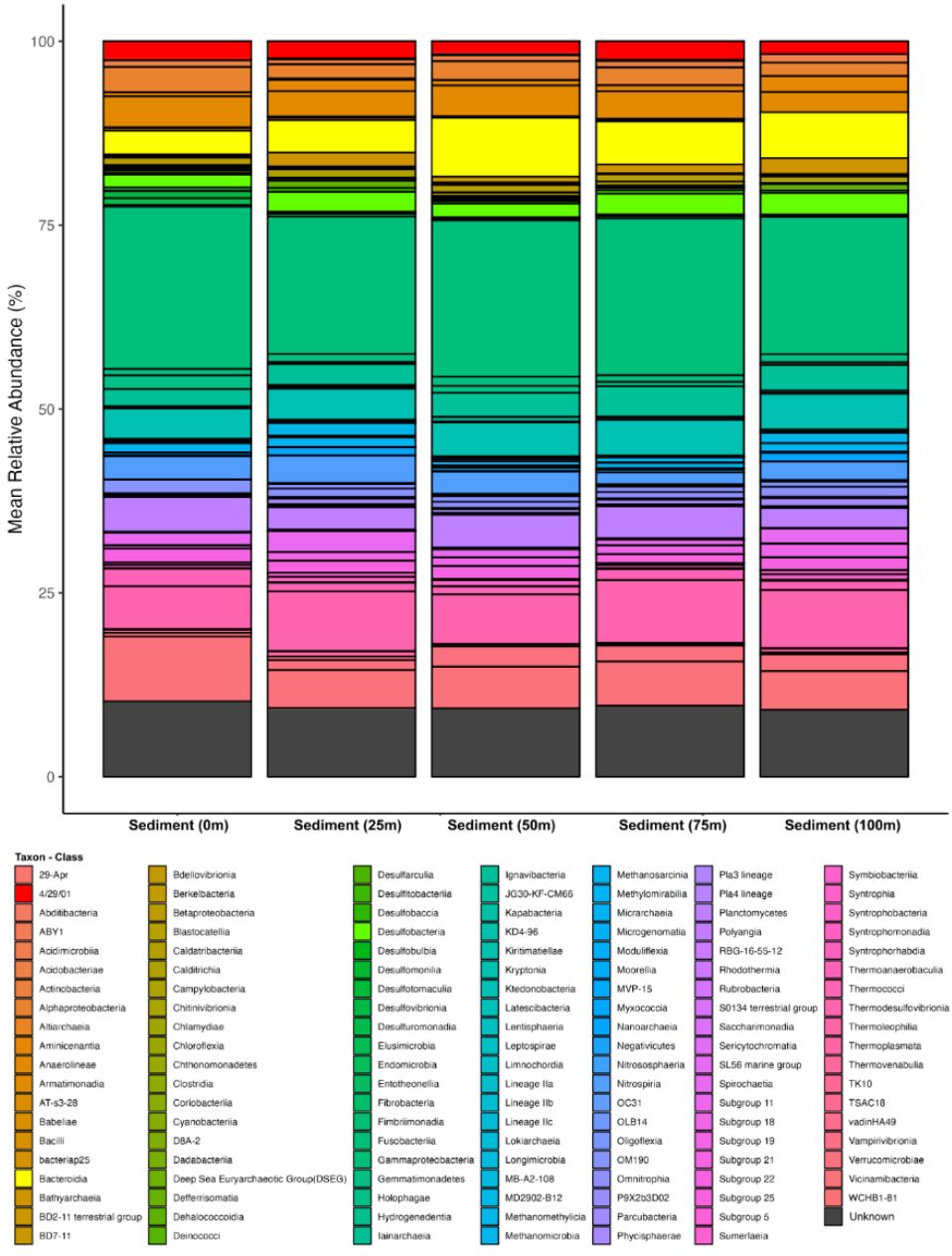

Figure 19. Class-level taxonomy barchart based on 16S rRNA gene sequencing data. Sediment samples showed to have similar mean relative abundances regardless of distance from wreck.

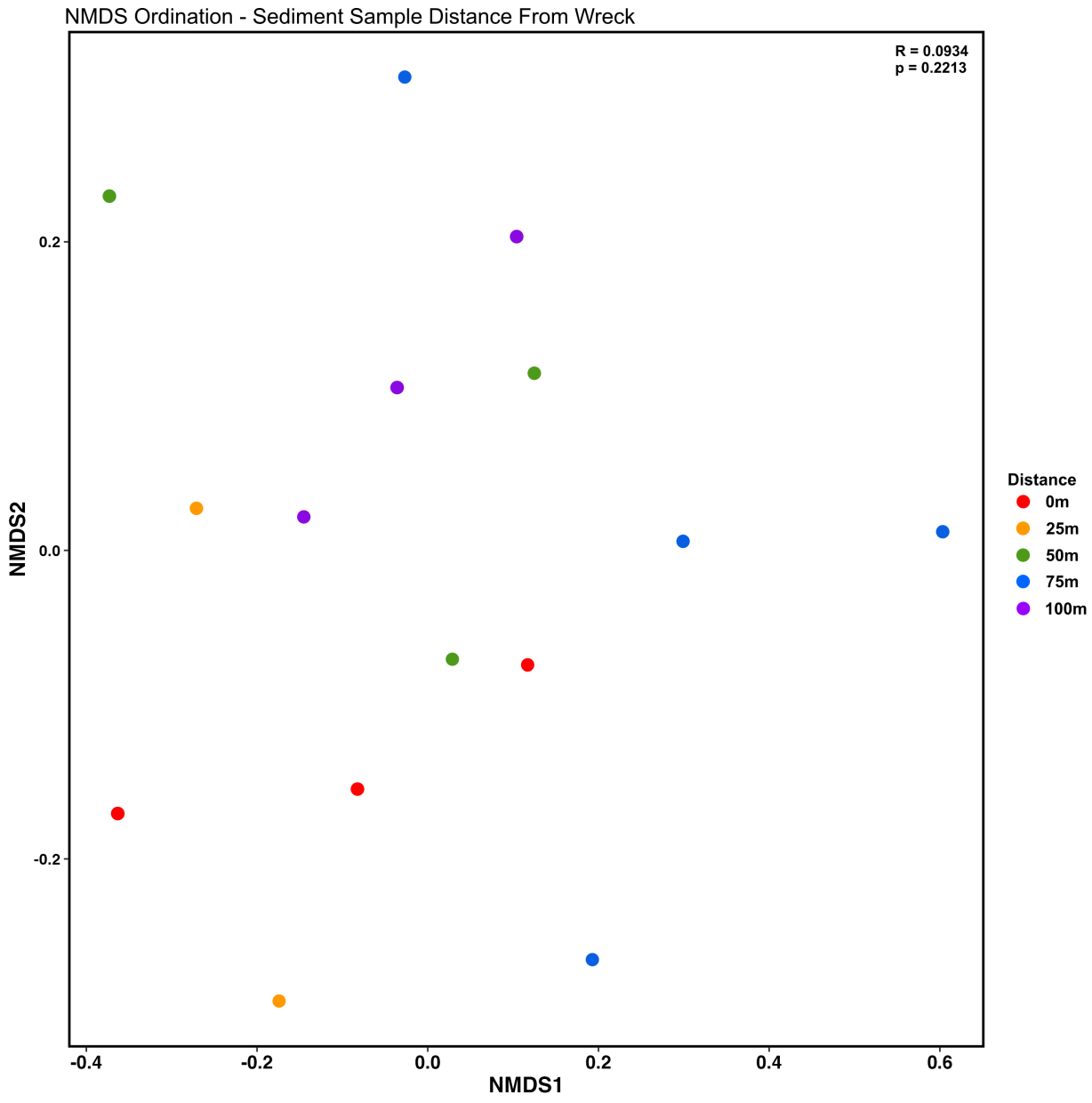

Figure 20. Non-metrical multidimensional ordination plot comparing various sediment samples at various distances away from the *Accomac* wreck. There was no statistically significant difference between microbial communities of the different sediment groups regardless of what distance from the wreck they were taken. Furthermore, the low R-value suggests microbial community members are similar in composition (ANOSIM: $R = 0.0934$; $p > 0.05$). Stress value of 0.09.

Comparison of Port Side vs Starboard Side of Wreck

Microbial communities located on the port side of the wreck had some overlap in grouping with starboard biofilm samples; however, there is no distinct separation between the communities (***Fig. 21***) There was still some dissimilarity between the microbial communities, specifically *Cyanobacteria* which comprise a higher mean relative abundance for starboard biofilm samples compared to port biofilm samples. This suggests a somewhat significant difference between the microbial community makeup between the port side of the ship and the starboard side, although, the difference is not as significant as all the different microenvironmetns compared to each other (*ANOSIM*: *R=0.2887*; *p=0.003*). The port side of the wreck had more wave action compared to the starboard side of the wreck, the slightly significant difference between the two sides of the wreck suggests that the increased wave action didn't influence the type of microbes that could form. Although, there was a higher quantity of biofim present on the starboard side of the ship compared to the port side. One explanation could be the increased wave action didn't allow suitable conditions for biofilm to aggregate as much on port side, but that the biofilm thickness did effect microbial community composition. This is an interesting finding and warrants further investigation in the future.

Surprisingly there was a statistically significant difference between Bow-Port, Bow-Starboard, Stern-Port, and Stern-Starboard biofilm samples (*ANOSIM*: *R=0.1684*, *p=0.0283*). This suggests that although the microbial communities don't differ from the left side of the wreck to the right side (Port vs Starboard), they do differ in community composition from the front of the wreck versus the back of the wreck. The phylum *Deinococcota* comprised of a higher abundance of port biofilm samples compared to starboard bioiflm samples, whereas the

phylum *Cyanobacteria* comprised of a higher abundance on starboard side (***Fig. 22***). This could be due to more sun exposure on starboard side compared to port side.

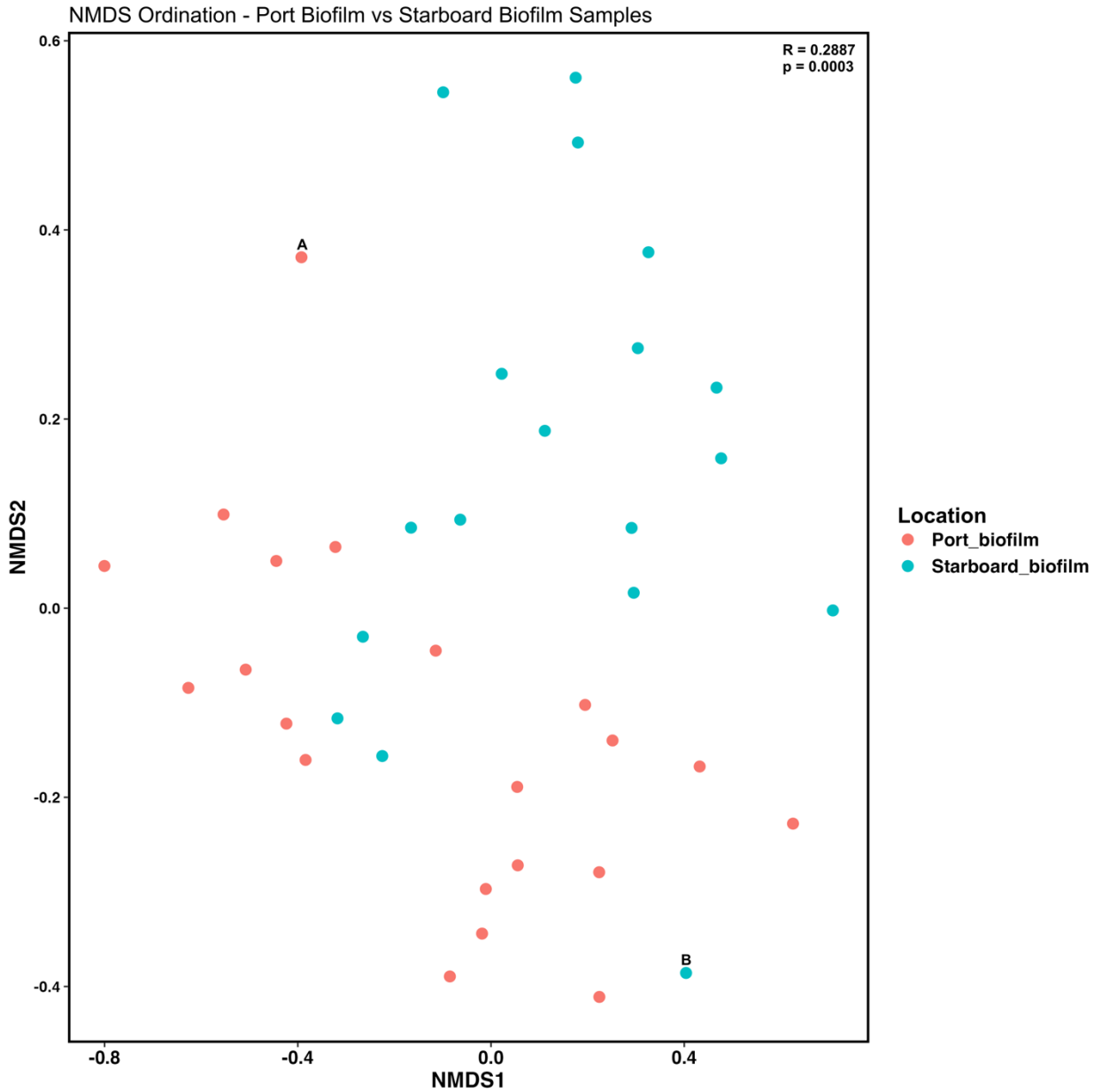

Figure 21. Non-metrical multidimensional ordination plot comparing port side biofilm samples and starboard biofilm samples. There was a statistically significant difference between port biofilm samples and starboard biofilm samples (ANOSIM: $R = 0.2887$, $p < 0.05$). Point A represents biofilm sample taken at bow of the wreck at the waterline. Point B represents starboard sample taken at the bow of the wreck but below the waterline. Stress value of 0.18.

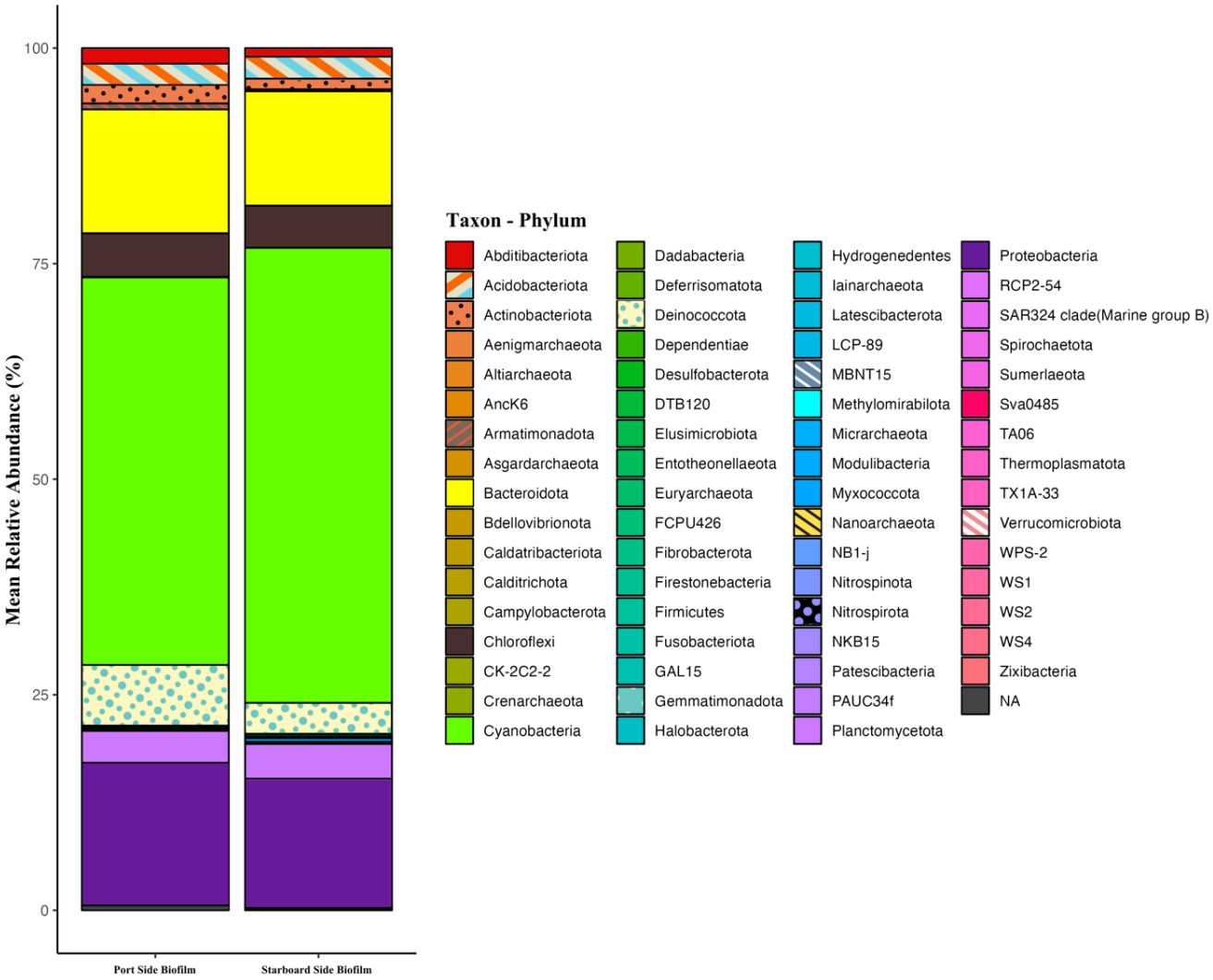

Figure 22. Phylum-level taxonomy barchart based on 16S rRNA gene sequencing data. Port side biofilm samples had similar mean relative abundance of taxon compared to the starboard biofilm samples. *Cyanobacteria* comprise most of the abundance for starboard shipwreck biofilm samples whereas *Deinococcota* comprised most of the abundance for port shipwreck biofilm samples.

Shipwreck biofilm samples were also separated based on whether they were sampled at the bow (front of wreck) compared to the stern (back of the wreck) (***Fig. 23***). There was no statistical difference between bo biofilm samples and stern biofilm samples, and the microbial community composition is similar between samples (*ANOSIM*: *R=0.02141*; *p=0.297*). To further analyze any potential differences between bow biofilm samples and stern biofilm samples, they

were subsequently divided into specific locations at which they were sampled (i.e., port vs starboard) (***Fig. 24***). Surprisingly, there was a statistically significant difference between microbial communities of Bow-Port, Bow-Starboard, Stern-Port and Stern-Starboard biofilm samples (ANOSIM: $R = 0.1684$, $p = 0.0283$). This difference in significant is interesting and warrants further analysis in the future.

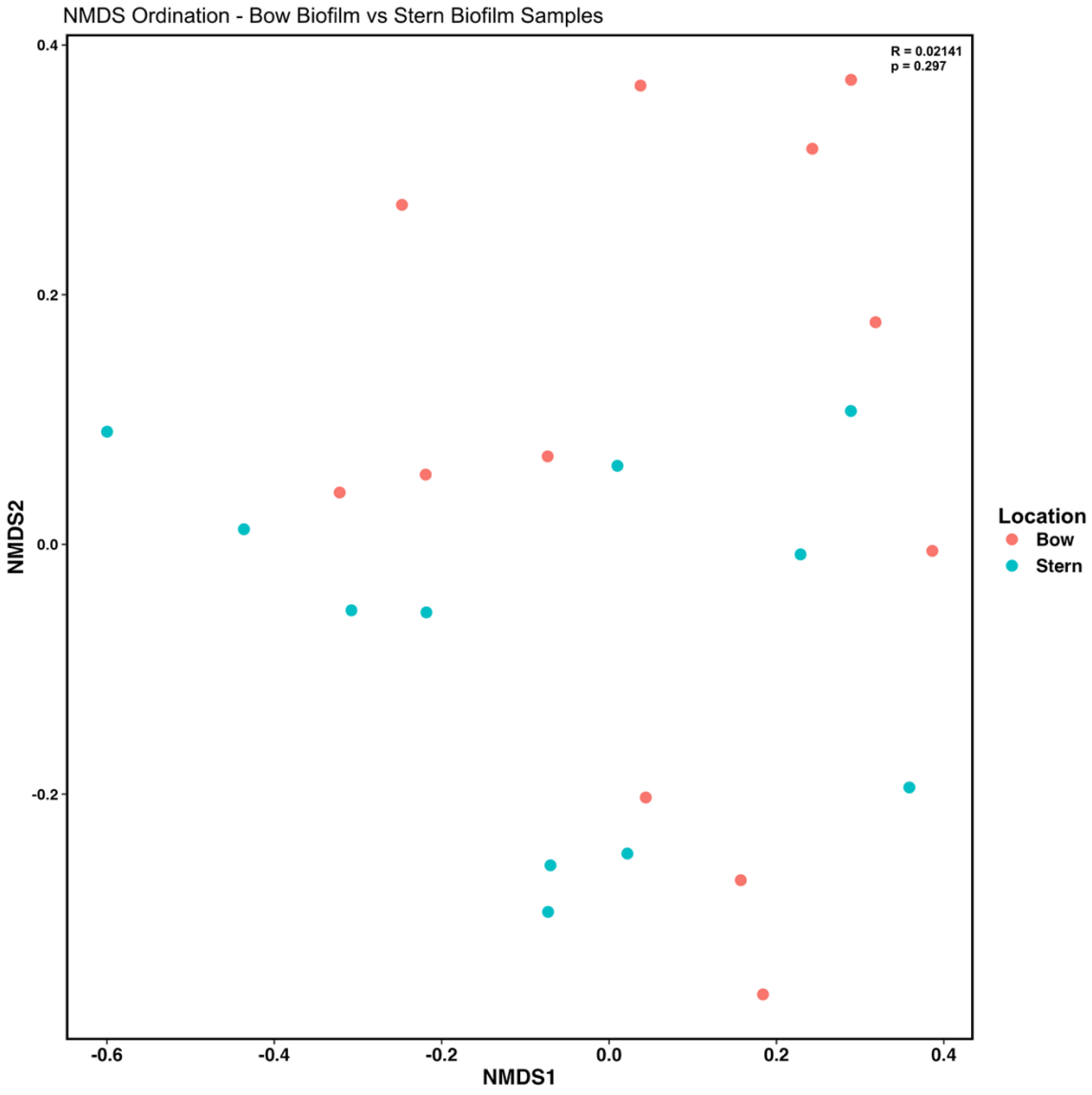

Figure 23. Non-metrical multidimensional ordination plot comparing bow biofilm samples to stern biofilm samples. There was no statistical difference between bow biofilm samples and stern biofilm samples, and the microbial community composition is similar between samples (ANOSIM: $R = 0.02141$, $p < 0.05$) Stress value of 0.17.

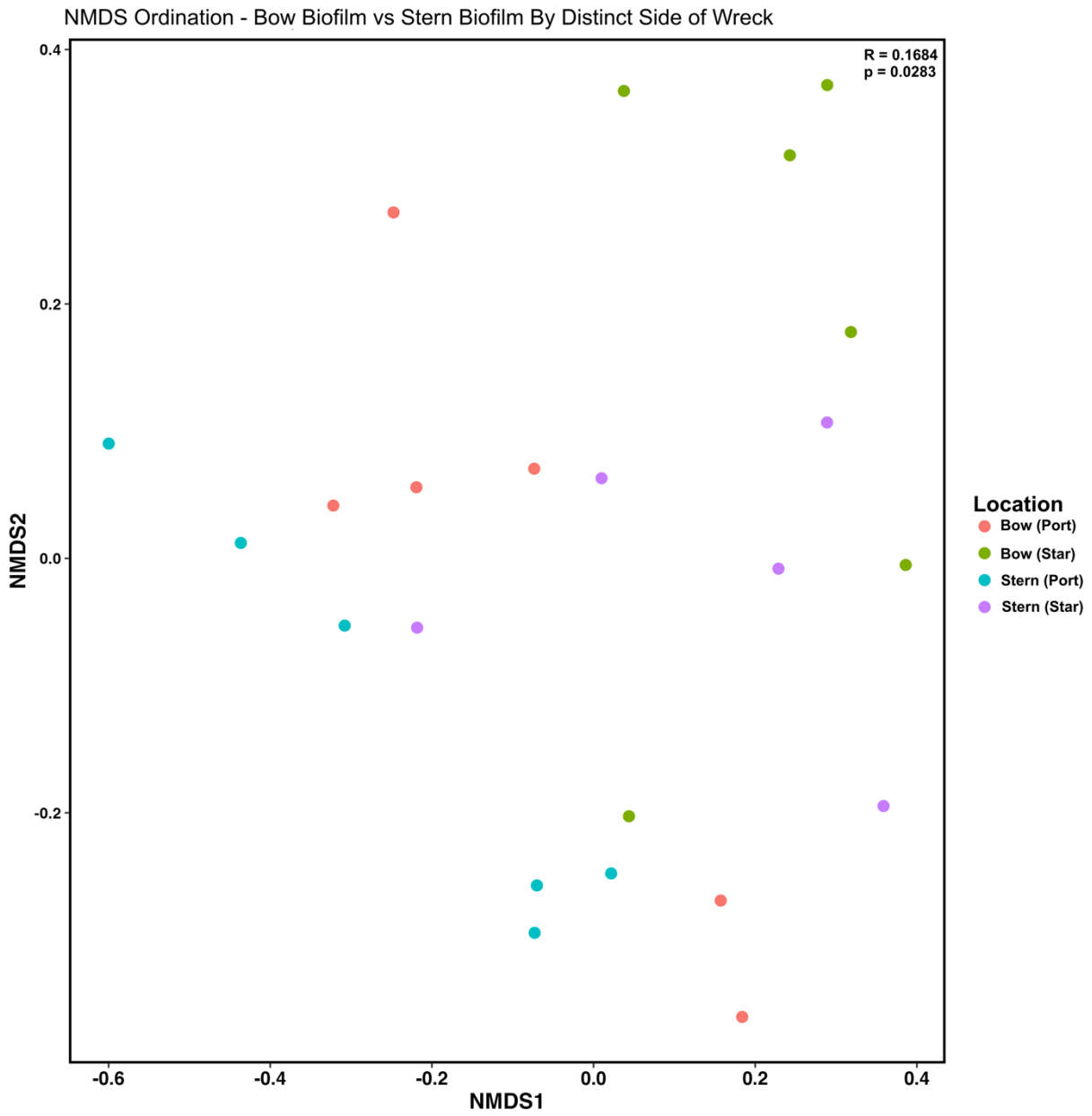

Figure 24. Non-metrical multidimensional ordination plot comparing bow biofilm samples taken on both port and starboard side to those at the stern on both port and starboard side. There was a statistically significant difference between microbial communities of Bow-Port, Bow-Starboard, Stern-Port and Stern-Starboard biofilm samples (ANOSIM: $R = 0.1684$, $p < 0.05$). Stress value of 0.17.

Water Depth Effects Microbial Composition

To determine if the location on the wreck, relative to the depth from the water surface, was a significant factor in microbial community composition, we analyzed samples based on their depths, specifically all biofilms sampled at 0ft (waterline) and 0.3ft (below waterline) (***Fig. 25***). Water depth was a statistically significant factor influencing the clustering of ASVs at the different sampling locations (ANOSIM: *R=0.4665*, *p=0.0001*). Overall, biofilms sampled at the waterline clustered separately from biofilms sampled below the waterline, except for outliers A, B, and C. Point A represents a biofilm sample taken at bow on starboard side, point B represents biofilm sample taken at the bulkhead and point C represents biofilm sample taken at the bow on port side. Outliers point A and point C were both taken at the bow of the ship, however on opposite sides of the wrecks. As determined previously, microbial biofilm community composition is influenced by the exact position of which the sample is taken from (i.e., bow sample taken on the port side vs stern sample taken on the starboard side). To determine if there was any variation in microbial community composition between the biofilm samples at the different depths, a stacked barchart was created at the phylum level (***Fig. 26***). There was a higher mean relative abundance of *Cyanobacteria* in biofilms sampled at a depth of 0ft (waterline) compared to biofilms sampled 0.3ft (below waterline). This is supported by the fact *Cyanobacteria* used sunlight for photosynthesis reactions, and those at the waterline have access to more light compared to those 0.3ft underwater. Alternatively, there was a higher relative abundance of *Proteobacteria* for biofilms sampled under the waterline compared to biofilms sampled at the waterline. There was a higher amount of biofilm formation, and corrosion, on samples under the waterline, which could suggest more activity from corrosion causing classes of Proteobacteria (i.e., *Betaproteobacteria* or *Gammaproteobacteria*)

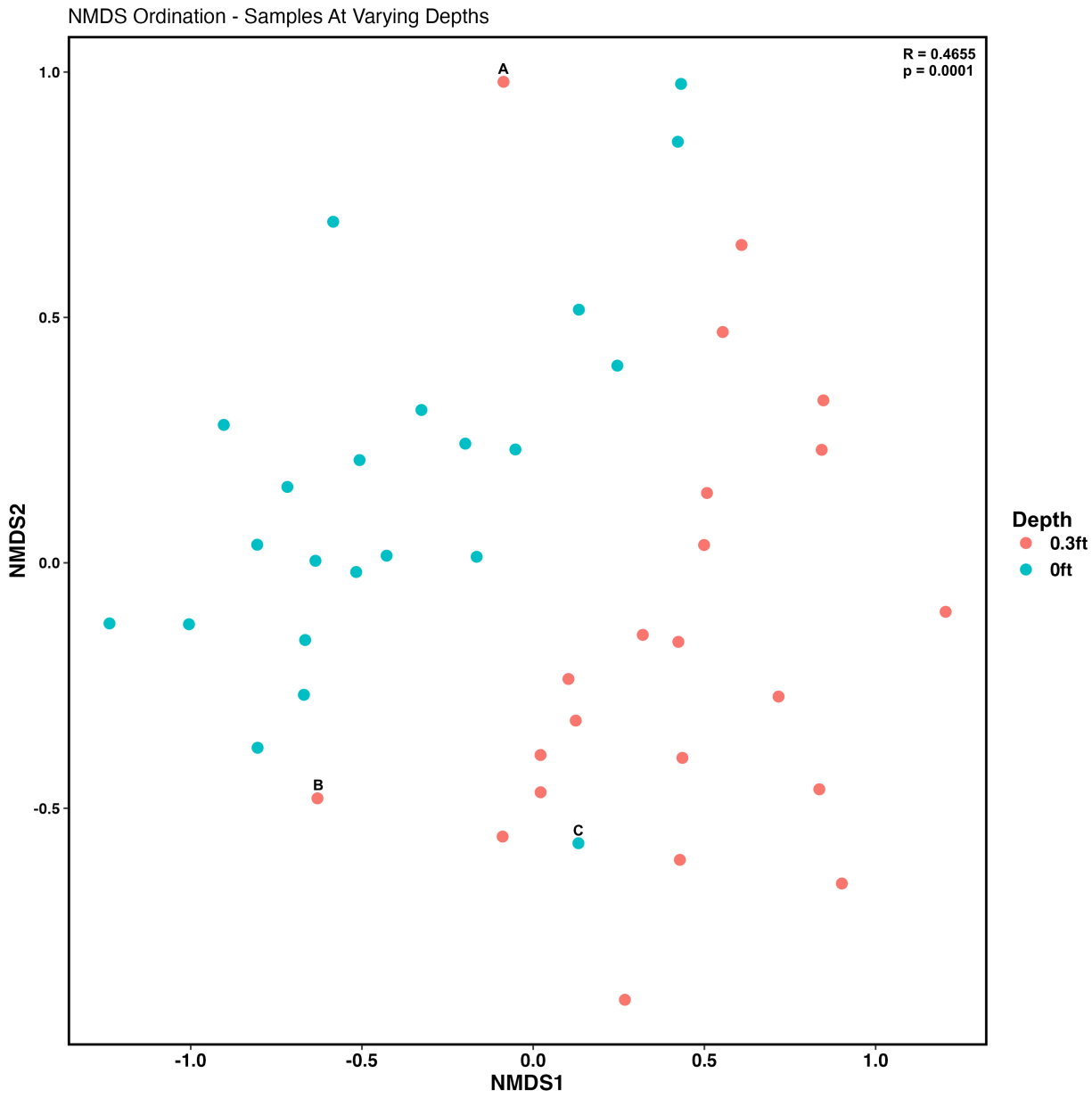

Figure 25. Non-metrical multidimensional ordination plot comparing various water depths of shipwreck biofilm samples, sediment samples and water samples. Point A represents a biofilm sample taken at bow on starboard side. Point B represents biofilm sample taken at the bulkhead. Point C represents biofilm sample taken at the bow on port side. There was a statistically significant difference between the different water depth of the samples (ANOSIM: $R = 0.6182$, $p < 0.05$). Stress value of 0.20.

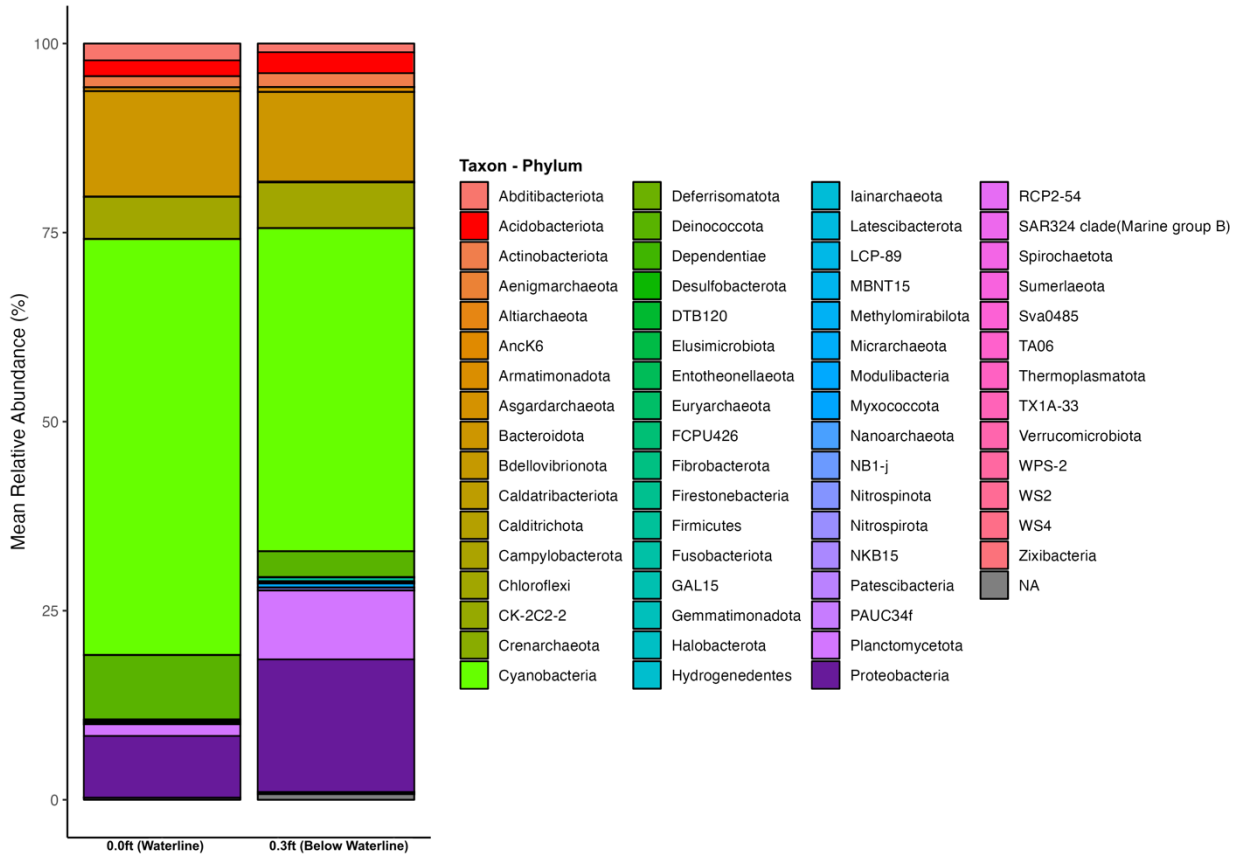

Figure 26. Phylum-level taxonomy barchart based on 16S rRNA gene sequencing data. Biofilm sample depth based on two measurements; waterline (0.0ft) and below waterline at (0.03ft). Mean relative abundance of various taxa differs between the two sampling depths.

Microbial Community Diversity of Shipwreck Site

Across The Entire Shipwreck Site

The Shannon H's diversity index was calculated to determine the taxonomic diversity between sampling groups and taxonomic variation within the groups themselves. The higher the Shannon H index, the more diverse the microbial communities are. Water samples had a higher average Shannon diversity index compared to shipwreck biofilm and sediment samples (***Fig. 27***). This suggests that microbial communities from this freshwater environment included more taxa in water samples, than for shipwreck biofilm and sediment samples.

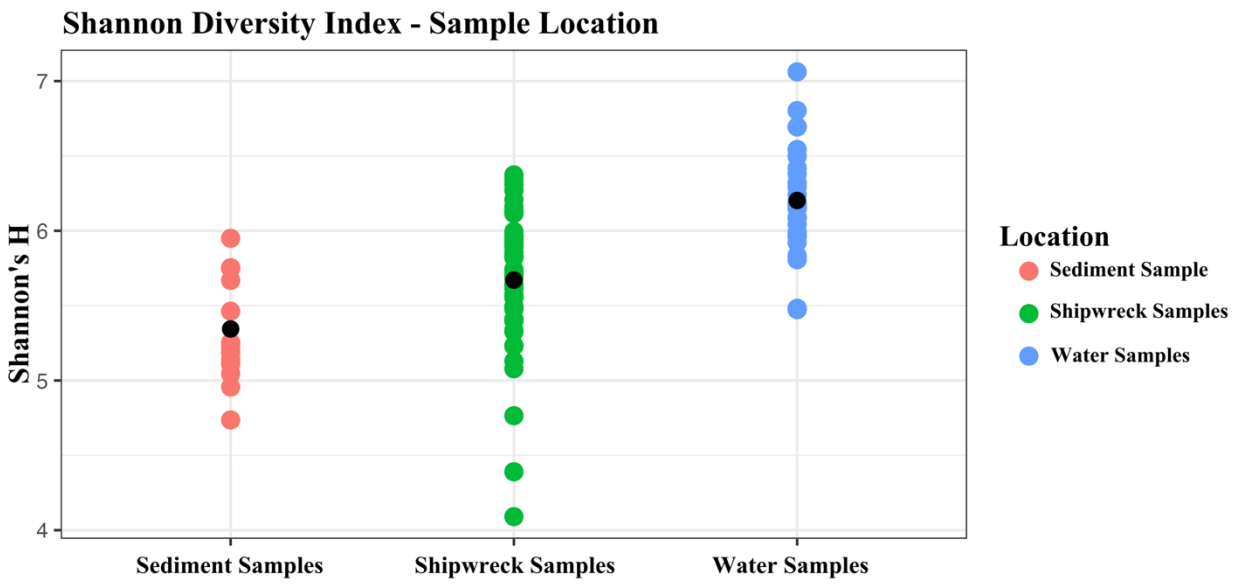

Figure 27. Shannon diversity indices plot of sediment samples, shipwreck biofilm samples and water samples. Their averages are represented by the black dots respectively (*5.34*, *5.67*, and *6.20*). Water samples had on average a higher Shannon's H index indicating they are more diverse in their taxonomic classification.

The diversity index for taxon richness was calculated to determine the number of ASV or individual taxa that are present for each sample; in other words, how many of each type of taxa there are. The water samples showed to have higher richness within the microbial communities compared to shipwreck biofilm samples and sediment samples (***Fig. 28***). This could be influenced by the mixing of water during high and low tides or by movement from the wind. Sediment samples were low in taxa richness but had high diversity indicating that although there are not a lot of members for each of the different taxa, there is a wide range of different taxa classifications.

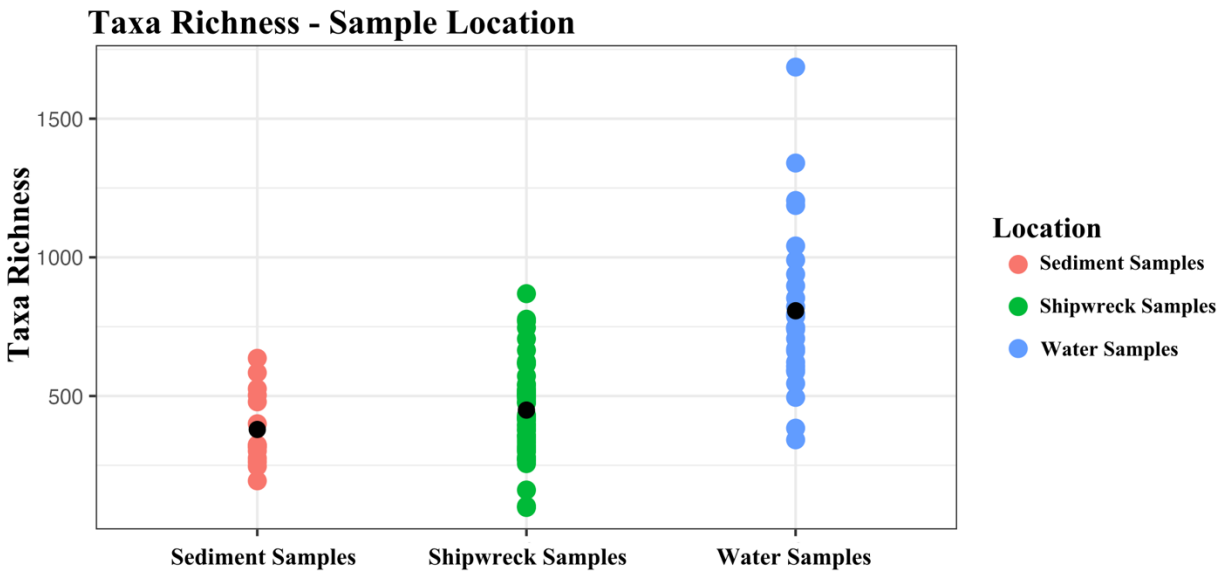

Figure 28. Taxa richness indices plot of sediment samples, shipwreck biofilm samples, and water samples. Black dots represent averages respectively (*379.37*, *449.21*, and *807.35*). Water samples had a larger spread in richness compared to sediment and shipwreck biofilm samples.

Pielou's evenness diversity index was calculated to determine if there was the same number of individuals for certain specified taxa within each different sampling group. Shipwreck biofilm samples were more varied in evenness compared to sediment and water samples (***Fig. 29***). Spread in evenness for sediment samples most likely is influenced by the distance from the shipwreck itself, as each sediment sample was taken in 25m increments west-east of the rudder post. This suggests that the microenvironment of the sediment changes as it is located further from the wreck. In summary, shipwreck biofilm microbial communities are greatly diverse and even in community composition but lack richness. Sediment samples, although moderately diverse, lack richness and evenness. Water samples have the greatest diversity and evenness but lack richness (***Fig. 30***).

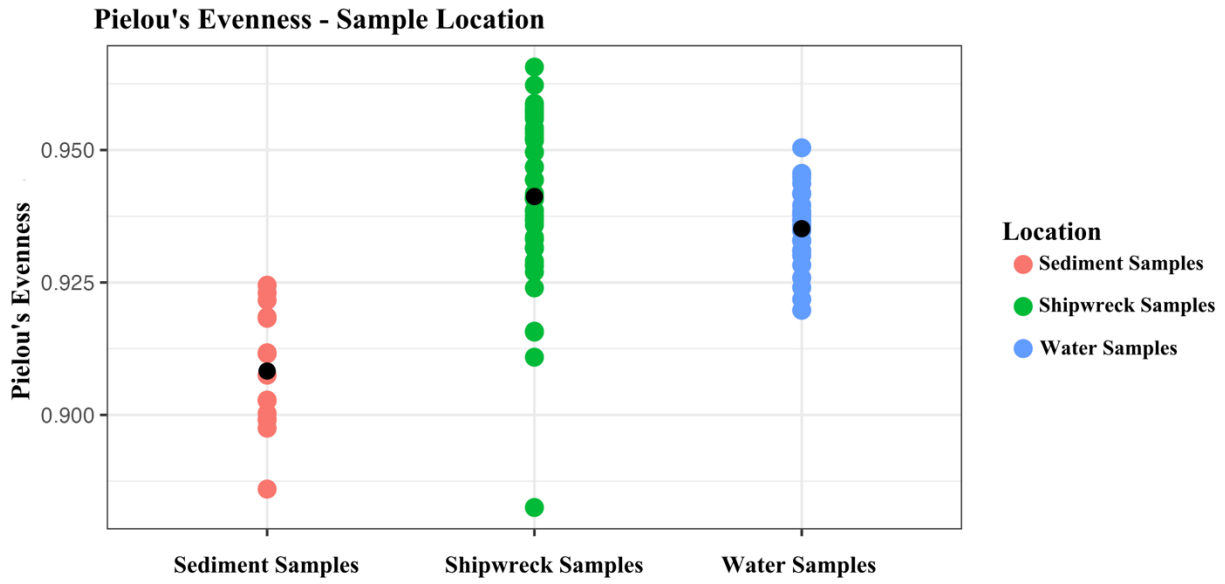

Figure 29. Pielou's evenness diversity index plot of sediment samples, shipwreck biofilm samples, and water samples. Black dots indicate averages respectively (*0.91*, *0.94*, and *0.94*). Shipwreck samples had the most spread in evenness and sediment samples had the least spread.

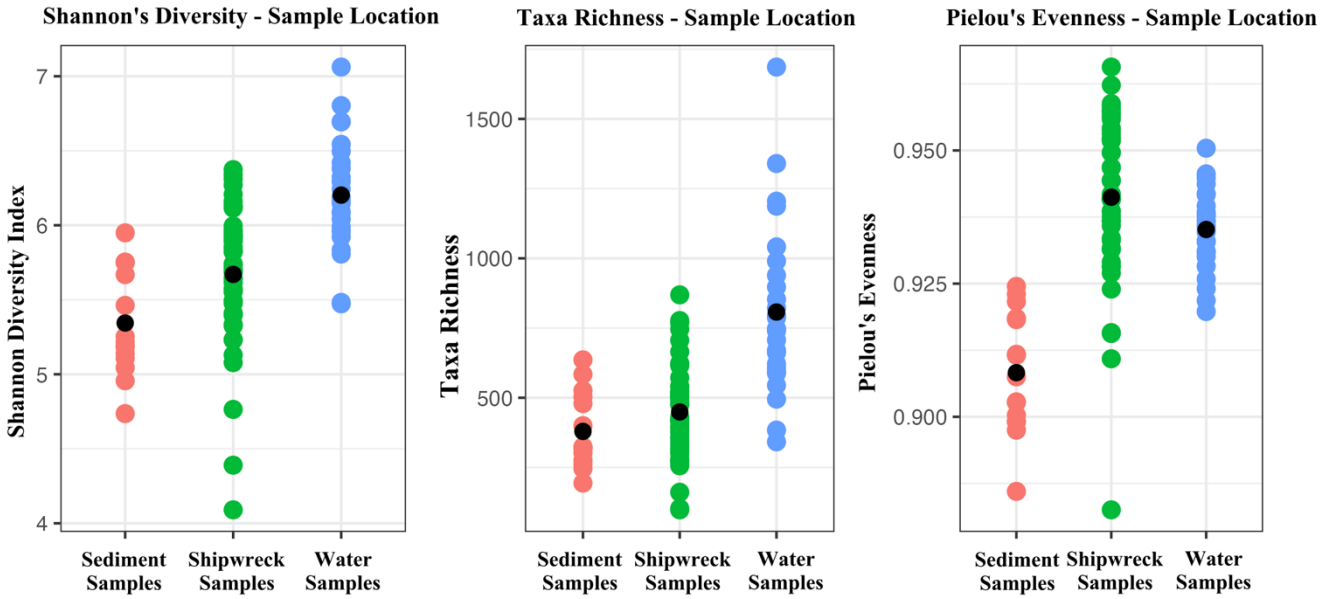

Figure 30. Shannon's H, taxa richness, and pielou's evenness diversity indices plots of sediment samples, shipwreck biofilm samples, and water samples. Black dots represent averages (see figures 15, 16 and 17 for values). Overall, sediment samples had moderate diversity, but low richness and evenness compared to water samples which had high diversity and evenness but low richness. Shipwreck biofilm samples had relatively high diversity and evenness, but low richness compared to water samples.

Port Side vs Starboard Side

Port biofilm samples (ave = *5.07;* ***Fig. 31***) had a similar Shannon's H diversity index to starboard biofilm samples (ave = *4.88*; ***Fig. 31***). The taxa richness index is relatively even between port biofilm samples (ave = 252.71; ***Fig. 32***) and starboard biofilm samples (ave = *214.56;* ***Fig. 32***). Pielou's evenness diversity induces has a larger spread for port biofilm samples compared to starboard biofilm samples, although their averages are relatively similar respectively (ave = 0.93, 0.92; ***Fig. 33***). Overall, these results indicates that microbial community diversity, was not affected by the distinct side of the wreck and each side has similar type and number of taxa (***Fig. 34***).

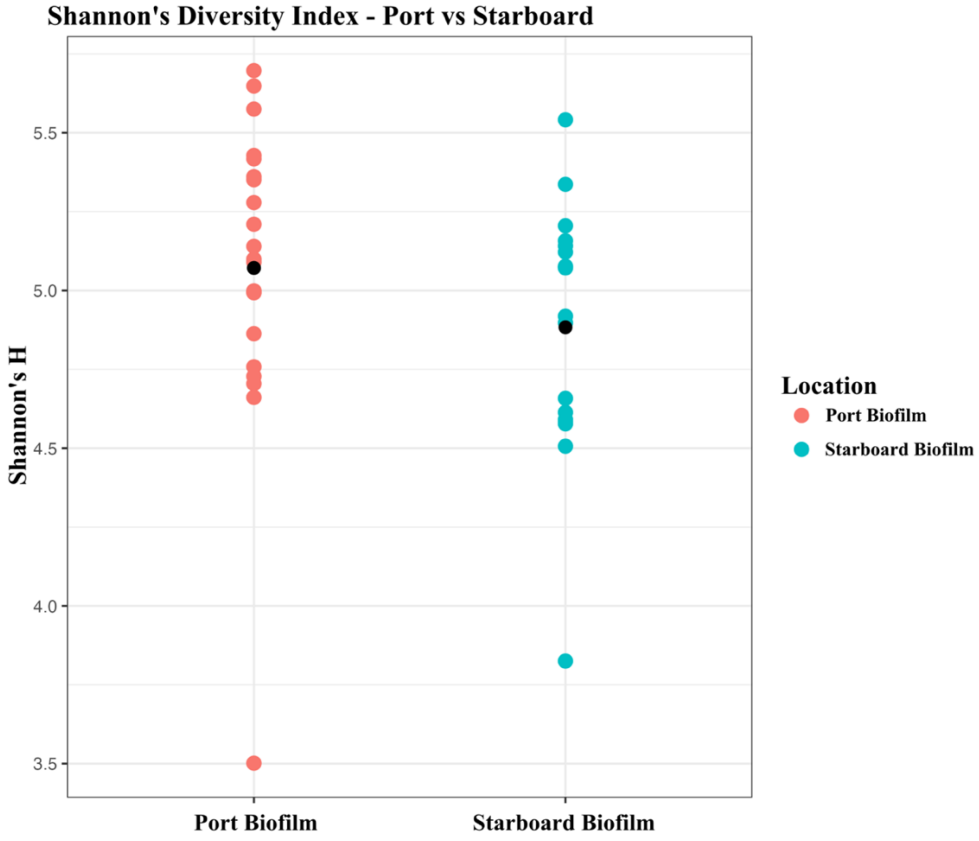

Figure 31. Shannon diversity indices plot of port biofilm samples and starboard biofilm samples. Their averages are represented by the black dots respectively (*5.07* and *4.88*). Diversity indices between port biofilm samples and starboard biofilm samples are relatively similar.

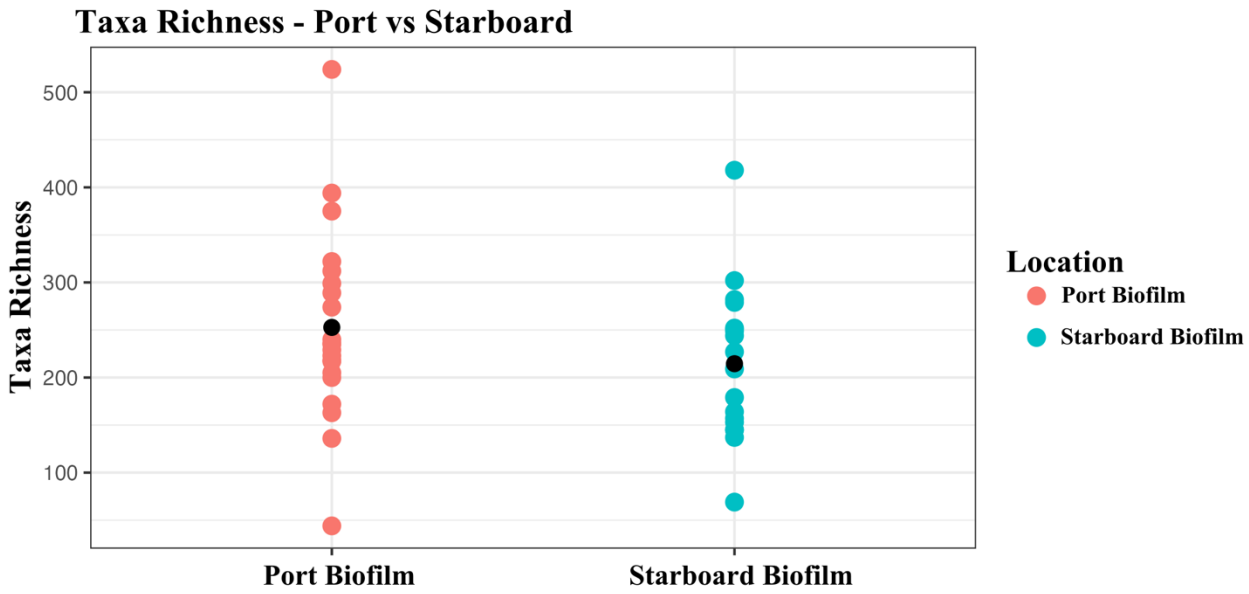

Figure 32. Species richness index plot of port biofilm samples and starboard biofilm samples. Black dots represent averages respectively (*252.71*, *214.56*). Port biofilms had a slightly wider spread of in species richness compared to starboard biofilm samples.

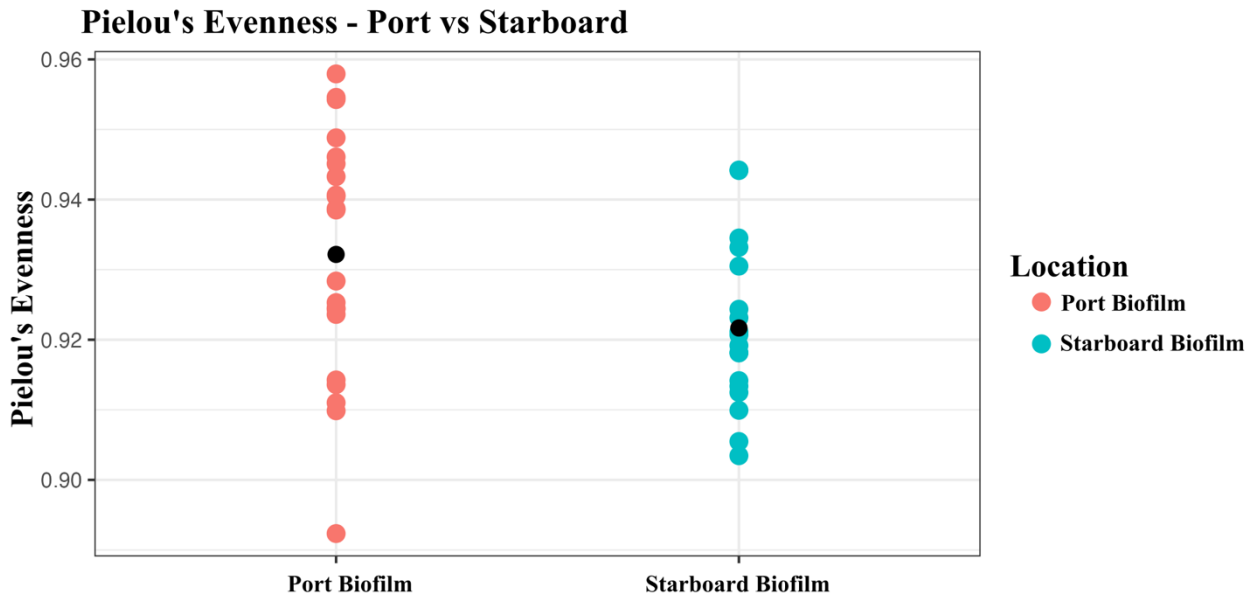

Figure 33. Pielou's evenness diversity index plot of port biofilm samples and starboard biofilm samples. Black dots indicate averages respectively (*0.93 and 0.92*). Port biofilm samples had a higher spread in evenness compared to starboard samples.

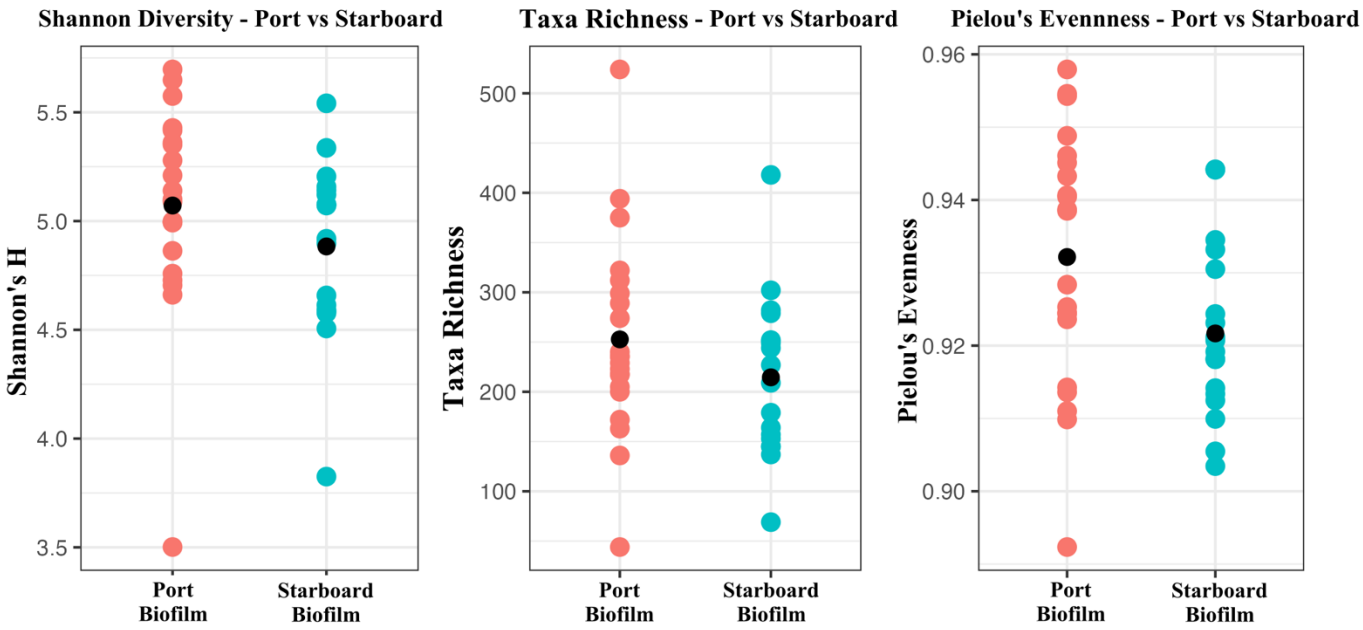

Figure 34. Shannon's H, species richness and pielou's evenness indices plots of port biofilm samples, and starboard biofilm samples. Black dots represent averages (*See Figures 19-21 for values*). Overall, port biofilm samples did not differ in diversity, richness, or evenness from starboard biofilm samples.

Identification of Corrosion Causing Taxa Across Wreck

Biocorrosion is mainly caused by the phylum *Betaproteobacteria* iron-oxidizers; however, sulfate-reducing bacteria also play a role. Of the samples sequenced, 61.2% of corrosion-causing ASV consisted of iron-oxidizers (***Table 3***). Seven genera of iron-oxidizers were identified on five separate sampling locations: port, starboard, after-quarters biofilm samples, sediment samples, and water samples. The specific genera identified by 16S rRNA sequencing include *Acidovorax*, *Bradyrhizobium*, *Dechloromonas*, *Ferritrophicum*, *Gallionella*, *Leptothrix*, and *Sideroxydans*. Although all genera were identified at each of the sampling locations, *Leptothrix* (*32.87%*) appeared more often across the wreck compared to *Sideroxydans* (*13.91%*) and *Ferritrophicum* (*4.89%*). The genera that appeared the least were *Acidovorax* (*4.43%*), *Dechloromonas* (*1.83%*), *Bradyrhizobium* (*2.60%*), and *Gallionella* (*0.61%*). Studies

suggest that these iron-oxidizers thrive in microaerophilic environments, those will low concentrations of oxygen (*Chan et al., 2016*; *Emerson et al., 2010*).

The sulfate reducers taxon is mainly comprised of the phylum *Deltaproteobacteria*, which is why it's included these phyla and their overall relative abundance with the different biofilm sampling locations in our analysis. Of the samples sequenced, 38.8% of corrosion-causing ASV sulfate-reducing bacteria (***Table 3***). The genera of known SRBs were identified in shipwreck biofilm samples from 16S rRNA sequencing: *Desulfobacca, Desulfomonile, Desulforegula, Desulfovibrio,* and *Desulfovirga* (*Thauer et al., 2007*). *Desulfobacca* (*18.50%*) and *Desulfovibrio* (*14.83%*) appeared the most often across the wreck compared to *Desulfomonile* (*3.06%*), *Desulforegula* (*0.61%*), and *Desulfovirga* (*1.83%*). Studies by Beech suggest that different genera of sulfate-reducing bacteria can influence corrosion rates; furthermore, different species of identical genera can cause variations in MIC regardless of similar environmental conditions (*Beech and Sunner, 2007*). Unlike iron-oxidizing bacteria, some genera of sulfate-reducing bacteria can thrive in aerobic environments (i.e., *Desulfovibrio*) whereas other genera, such as *Desulfobacter*, are restricted to anaerobic environments (*Sass et al., 2007*).

Enrichment cultures were created, and DNA was extracted for sequencing to determine if FeOB bacteria would be identified for comparison against previous 16S rRNA sequencing of the shipwreck biofilm samples (*See Meredith Cox Honors Thesis for methods*). All SRB genera identified in the shipwreck biofilm samples were not consecutively identified in the enrichment culture samples, this suggests the media did not provide substantial nutritional requirements nor the necessary environmental conditions for growth (***Table 4***). Of the iron-oxidizing bacteria identified from the shipwreck biofilm sequencing, only *Bradyrhizobium*, *Dechloromonas*,

Gallionella, and *Sideroxydans* were also identified in the enrichment cultures. Surprisingly, *Acidovorax* was not identified from the original biofilm sequencing samples but was then later identified during the enrichments. This could suggest a low abundance of thus genus present in the biofilm sample sent for sequencing was under the threshold for identification, compared to the enrichment sample.

Table 3. Identification of total percentage of corrosion causing taxa: iron-oxidizing bacteria (orange) and sulfate-reducing bacteria (purple). Count represents number of corrosion causing taxa out of 654 total applicable ASVs from various sampling locations.

Genus	After Quarters Biofilm	Port Biofilm	Starboard Biofilm	Total %
Acidovorax	8	14	7	4.43
Bradyrhizobium	5	8	4	2.60
Dechloromonas	3	6	3	1.83
Desulfobacca	34	58	29	18.50
Desulfomonile	5	10	5	3.06
Desulforegula	1	2	1	0.61
Desulfovibrio	25	48	24	14.83
Desulfovirga	3	6	3	1.83
Ferritrophicum	8	16	8	4.89
Gallionella	1	2	1	0.61
Leptothrix	59	104	52	32.87
Sideroxydans	28	42	21	13.91

Table 4. Comparison of identification of iron-oxidizing (orange) taxa and sulfate-reducing (purple) taxa identified from shipwreck biofilm sample sequencing results and enrichment culture sequencing.

FeOB Genera	Presence in Biofilm Sequencing	Presence in Enrichment Culture Sequencing
Acidovorax	No	Yes
Bradyrhizobium	Yes	Yes
Dechloromonas	Yes	Yes
Desulfobacca	Yes	No
Desulfomonile	Yes	No
Desulforegula	Yes	No
Desulfovibrio	Yes	No
Desulfovirga	Yes	No
Ferritrophicum	Yes	No
Gallionella	Yes	Yes
Leptothrix	Yes	No
Sideroxydans	Yes	Yes

CONCLUSION & FUTURE DIRECTIONS

This study aimed to determine if microbial community diversity and relative abundance varied across the shipwreck *Accomac* located in Mallows Bay, Maryland. Microenvironments play a significant role in determining what microbial species can survive and thrive on this ferrous-hulled structure. Our results were supported by biofilm community makeup findings on steel coupons in similar ecosystems (*Hicks, 2007*). Our hypothesis of water depth playing a significant role in biofilm community composition was supported as we saw clustering of ASVs of similar depths and distinct clustering between the two depths samples were taken at. Corrosion causing taxa were identified across the entirety of the wreck regardless of the surrounding environment; however, we cannot conclude that the identified FeOBs and SRBs are responsible for the corrosion seen across the wreck. Further analysis would be needed of those bacteria using RNA-based analysis methods. Lastly, there were similar trends in microbial community member assemblages in this freshwater system compared to trends found in marine systems in terms of the microbial biofilm communities' suggesting that the microenvironment influences community composition within a wreck site (*Price et al., 2020; Garrison et al., 2019).* Likewise, research by *Alonso-Sáez et al*. corroborates the abundance of freshwater iron-oxidizing *Betaproteobacteria* in strictly freshwater systems – which also suggests metabolic activity of those organisms (*McBeth and Emerson, 2016*).

Additional analysis and research on biofilm formation in freshwater, and shallow systems will allow for microbial community trend comparison against biofilm formation in marine environments through increased sampling. Through this comparison, knowledge about the potential influences the forming biofilm community has on the surrounding ecosystem and ferrous structures will be obtained. To preserve *Accomac*, and thus other shipwrecks in

freshwater environments, it is suggested that microbial sampling be completed every few years to determine if there is any shift in microbial composition. Persistent investigation of biofilm formation on ferrous-hull structures through sampling and collaboration, will allow researchers to further understand the effects microbes have on these systems. Thus, preservation plans can be put in place to conserve what is left of these magnificent structures that not only tell a story of time but allow a new community to develop and thrive.

REFERENCES

1. Anderson, M.J.; Walsh, D.C.I. PERMANOVA, ANOSIM, and the Mantel test in the face of heterogeneous dispersions: What null hypothesis are you testing? *Ecol. Monogr.* **2013**, *83*, 557–574.

2. Beech IB, Sunner JA, Hiraoka K. Microbe-surface interactions in biofouling and biocorrosion processes. In: *International Microbiology*. Vol 8. ; 2005. doi:10.2436/im.v8i3.9522

3. Beech IB, Sunner JA. Sulphate-reducing bacteria and their role in corrosion of ferrous materials. *Sulphate-reducing Bacteria: Environmental and Engineered Systems*. 2007; 558:484-507

4. Begmatov S, Beletsky A V., Dedysh SN, Mardanov A V., Ravin N V. Genome analysis of the candidate phylum MBNT15 bacterium from a boreal peatland predicted its respiratory versatility and dissimilatory iron metabolism. *Front Microbiol*. 2022;13(August):1-14. doi:10.3389/fmicb.2022.951761

5. Besemer K. Europe PMC Funders Group Biodiversity , community structure and function of biofilms in stream ecosystems. *Res Microbiol*. 2016;166(10):774-781. doi:10.1016/j.resmic.2015.05.006.Biodiversity

6. Blumwald E, Tel-Or E. Salt adaptation of the cyanobacterium synechococcus 6311 growing in a contin- uous culture (turbidostat). Plant Physiol. 1984; 74(1):183–5. PMID: 16663376

7. Brock M. The Effect of Historic Shipwrecks on Sediment Microbiomes in the Northern Gulf of Mexico by. Published online 2019.

8. Callahan BJ, McMurdie PJ, Rosen MJ, Han AW, Johnson AJA, Holmes SP. Dada2: High resolution sample inference from Illumina amplicon data. *Encycl Med Immunol*. 2016;13(7):1-7. doi:10.1007/978-1-4614-9209-2_118-1

9. Callahan BJ, McMurdie PJ, Holmes SP. Exact sequence variants should replace operational taxonomic units in marker-gene data analysis. *ISME J*. 2017;11(12):2639-2643. doi:10.1038/ismej.2017.119

10. Chan CS, Emerson D, Luther GW. The role of microaerophilic Fe-oxidizing micro-organisms in producing banded iron formations. *Geobiology*. 2016;14(5):509-528. doi:10.1111/gbi.12192

11. Comeau AM, Li WKW, Tremblay JÉ, Carmack EC, Lovejoy C. Arctic ocean microbial community structure before and after the 2007 record sea ice minimum. *PLoS One*. 2011;6(11). doi:10.1371/journal.pone.0027492

12. Comeau AM, Douglas GM & Langille MG (2016) Microbiome helper: a custom and streamlined workflow for microbiome research. *MSystems* 2: e00127-00116.

13. Dobretsov S, Coutinho R, Rittschof D, Salta M, Ragazzola F, Hellio C. The oceans are changing: impact of ocean warming and acidification on biofouling communities. *Biofouling*. 2019;35(5):585-595. doi:10.1080/08927014.2019.1624727

14. Donlan RM. Biofilms: Microbial life on surfaces. *Emerg Infect Dis*. 2002;8(9). doi:10.3201/eid0809.020063

15. Dubiel M, Hsu CH, Chien CC, Mansfeld F, Newman DK. Microbial iron respiration can protect steel from corrosion. *Appl Environ Microbiol*. 2002;68(3). doi:10.1128/AEM.68.3.1440-1445.2002

16. Emerson D, Fleming EJ, McBeth JM. Iron-oxidizing bacteria: An environmental and genomic perspective. *Annu Rev Microbiol*. 2010;64:561-583. doi:10.1146/annurev.micro.112408.134208

17. Emerson D. The role of iron-oxidizing bacteria in biocorrosion: a review. *Biofouling*. 2019;34(9):989-1000. doi:10.1080/08927014.2018.1526281

18. Enning D, Garrelfs J. Corrosion of iron by sulfate-reducing bacteria: New views of an old problem. *Appl Environ Microbiol*. 2014;80(4). doi:10.1128/AEM.02848-13

19. De França FP, Ferreira CA, Lutterbach MTS. Effect of different salinities of a dynamic water system on biofilm formation. *J Ind Microbiol Biotechnol*. 2000;25(1):45-48. doi:10.1038/sj.jim.7000020

20. Fry I V., Huflejt M, Erber WWA, Peschek GA, Packer L. The role of respiration during adaptation of the freshwater cyanobacterium Synechococcus 6311 to salinity. *Arch Biochem Biophys*. 1986;244(2):686-691. doi:10.1016/0003-9861(86)90637-5

21. Garrison CE, Price KA, Field EK. Environmental Evidence for and Genomic Insight into the Preference of Iron-Oxidizing Bacteria for More-Corrosion-Resistant Stainless Steel at Higher Salinities. *Appl Environ Microbiol*. 2019;85(14):1-14. doi:10.1128/AEM.00483-19

22. Garrison CE, Field EK. Introducing a “core steel microbiome” and community functional analysis associated with microbially influenced corrosion. *FEMS Microbiol Ecol*. 2021;97(1). doi:10.1093/femsec/fiaa237

23. Glassman SI & Martiny JB (2018) Broadscale ecological patterns are robust to use of exact sequence variants versus operational taxonomic units. *MSphere* 3: e00148- 00118.

24. Hahnke RL, Meier-Kolthoff JP, García-López M, et al. Genome-based taxonomic classification of Bacteroidetes. *Front Microbiol*. 2016;7(DEC). doi:10.3389/fmicb.2016.02003

25. Hamdan LJ, Salerno JL, Reed A, Joye SB, Damour M. The impact of the Deepwater Horizon blowout on historic shipwreck-associated sediment microbiomes in the northern Gulf of Mexico. *Sci Rep*. 2018;8(1):1-14. doi:10.1038/s41598-018-27350-z

26. Hamdan LJ, Hampel JJ, Moseley RD, et al. Deep-sea shipwrecks represent island-like ecosystems for marine microbiomes. *ISME J*. 2021;15(10):2883-2891. doi:10.1038/s41396-021-00978-y

27. Hampel JJ, Moseley RD, Hamdan LJ. Microbiomes respond predictably to built habitats on the seafloor. *Mol Ecol*. Published online 2022:0-2. doi:10.1111/mec.16504

28. Hedrich S, Schlömann M, Barrie Johnson D. The iron-oxidizing proteobacteria. *Microbiology*. 2011;157(6):1551-1564. doi:10.1099/mic.0.045344-0

29. Henri PA, Rommevaux-Jestin C, Lesongeur F, et al. Structural iron (II) of basaltic glass as an energy source for zetaproteobacteria in an abyssal plain environment, off the mid-atlantic ridge. *Front Microbiol*. 2016;6(JAN). doi:10.3389/fmicb.2015.01518

30. Johnson DL, Wilson BM, Carr JD, Russell MA, Murphy LE, Conlin DL. Corrosion of steel shipwreck in the marine environment: USS Arizona - Part 1. *Mater Perform*. 2006;45(10):40-44.

31. Kchouk M, Gibrat JF, Elloumi M. Generations of Sequencing Technologies: From First to Next Generation. *Biol Med*. 2017;09(03). doi:10.4172/0974-8369.1000395

32. Khomich M, Måge I, Rud I, Berget I. Analysing microbiome intervention design studies: Comparison of alternative multivariate statistical methods. *PLoS One*. 2021;16(11 November):1-20. doi:10.1371/journal.pone.0259973

33. Kielak AM, Barreto CC, Kowalchuk GA, van Veen JA, Kuramae EE. The ecology of Acidobacteria: Moving beyond genes and genomes. *Front Microbiol*. 2016;7(MAY):1-16. doi:10.3389/fmicb.2016.00744

34. Kim Y, Jeon J, Kwak MS, Kim GH, Koh IS, Rho M. Photosynthetic functions of Synechococcus in the ocean microbiomes of diverse salinity and seasons. *PLoS One*. 2018;13(1):4-8. doi:10.1371/journal.pone.0190266

35. Loman NJ, Misra R V., Dallman TJ, et al. Performance comparison of benchtop high-throughput sequencing platforms. *Nat Biotechnol*. 2012;30(5). doi:10.1038/nbt.2198

36. Marsili, E., Kjelleberg, S., & Rice, S. A. (2018). Mixed community biofilms and microbially influenced corrosion. Microbiology Australia, 39(3), 152-157. doi:10.1071/MA18046

37. Martijn J, Vosseberg J, Guy L, Offre P, Ettema TJG. Letter. *Nature*. Published online 2018. http://dx.doi.org/10.1038/s41586-018-0059-5%0Ahttp://dx.doi.org/10.1038/s41586-018-0086-2

38. Mcbeth JM, Fleming EJ, Emerson D. The transition from freshwater to marine iron-oxidizing bacterial lineages along a salinity gradient on the Sheepscot River, Maine, USA. *Environ Microbiol Rep*. 2013;5(3). doi:10.1111/1758-2229.12033

39. McMurdie PJ & Holmes S (2013) phyloseq: an R package for reproducible interactive analysis and graphics of microbiome census data. *PloS one* 8: e61217.

40. Melchers RE. Microbiological and abiotic processes in modelling longer-term marine corrosion of steel. *Bioelectrochemistry*. 2014;97. doi:10.1016/j.bioelechem.2013.07.002

41. Mehrshad M, Salcher MM, Okazaki Y, et al. Hidden in plain sight—highly abundant and diverse planktonic freshwater Chloroflexi. *Microbiome*. 2018;6(1):1-13. doi:10.1186/s40168-018-0563-8

42. Moreno DA, Ibars JR, Polo JL, Bastidas JM. EIS monitoring study of the early microbiologically influenced corrosion of AISI 304L stainless steel condenser tubes in freshwater. *J Solid State Electrochem*. 2014;18(2). doi:10.1007/s10008-014-2390-6

43. Morris EK, Caruso T, Buscot F, et al. Choosing and using diversity indices: Insights for ecological applications from the German Biodiversity Exploratories. *Ecol Evol*. 2014;4(18). doi:10.1002/ece3.1155

44. Mugge RL, Brock ML, Salerno JL, et al. Deep-sea biofilms, historic shipwreck preservation and the Deepwater Horizon spill. *Front Mar Sci*. 2019;6(FEB). doi:10.3389/fmars.2019.00048

45. Nakayama Y, Yamaguchi H, Einaga N, Esumi M. Pitfalls of DNA quantification using dnabinding fluorescent dyes and suggested solutions. *PLoS One*. 2016;11(3). doi:10.1371/journal.pone.0150528

46. Oksanen J, Blanchet GF, Friendly M*, et al.* (2017) vegan: Community Ecology Package. R package version 2.4-4.

47. Peng CG, Park JK, Patenaude RW. Statistics-based classification of microbially influenced corrosion in freshwater systems. *Water Res*. 1994;28(4). doi:10.1016/0043-1354(94)90104-X

48. Price KA, Garrison CE, Richards N, Field EK. A Shallow Water Ferrous-Hulled Shipwreck Reveals a Distinct Microbial Community. *Front Microbiol*. 2020;11. doi:10.3389/fmicb.2020.01897

49. Quast, C., Pruesse, E., Yilmaz, P., Gerken, J., Schweer, T., Yarza, P., et al. (2013). The SILVA ribosomal RNA gene database project: Improved data processing and web-based tools. *Nucleic Acids Res*. 41, D590–D596. doi: 10.1093/nar/gks1219

50. R Development Core Team (2017) R: A language and environment for statistical computing. R Foundation for Statistical Computing, Vienna, Austria.

51. Sass H, Cypionka, H. Response to sulphate-reducing bacteria to oxygen. *Sulphate-reducing Bacteria: Environmental and Engineered Systems*. 2007; 558:187-203

52. Shomette DD. *The Shipwrecks of Mallows Bay: A Historic Overview*.; 1998.

53. Shomette DD. *The Shipwrecks of Mallows Bay: Inventory & Assessment*.; 1998.

54. Swanson KL. *Crabs & 'crobes: The tripartite relationship of a host, parasite, and their respective microbiomes.* East Carolina University; 2020.

55. Telegdi J, Shaban A, Trif L. Microbiologically influenced corrosion (MIC). *Trends Oil Gas Corros Res Technol Prod Transm*. 2017;(Mic):191-214. doi:10.1016/B978-0-08-101105-8.00008-5

56. Thauer RK, Stackebrandt E, Hamilton WA. Energy metabolism and phylogenetic diversity of sulphate-reducing bacteria. *Sulphate-reducing Bacteria: Environmental and Engineered Systems*. 2007; 558:21-58

57. Usher KM, Kaksonen AH, Cole I, Marney D. Critical review: Microbially influenced corrosion of buried carbon steel pipes. *Int Biodeterior Biodegrad*. 2014;93:84-106. doi:10.1016/j.ibiod.2014.05.007

58. Venzlaff H, Enning D, Srinivasan J, et al. Accelerated cathodic reaction in microbial corrosion of iron due to direct electron uptake by sulfate-reducing bacteria. *Corros Sci*. 2013;66. doi:10.1016/j.corsci.2012.09.006

59. Vigneron A, Head IM, Tsesmetzis N. Damage to offshore production facilities by corrosive microbial biofilms. *Appl Microbiol Biotechnol*. 2018;102(6). doi:10.1007/s00253-018-8808-9

60. Vineis P, Chan Q, Khan A. Climate change impacts on water salinity and health. *J Epidemiol Glob Health*. 2011;1(1):5-10. doi:10.1016/j.jegh.2011.09.001

61. Vinogradova N, Lee T, Boutin J, et al. Satellite Salinity Observing System: Recent Discoveries and the Way Forward. *Front Mar Sci*. 2019;6. doi:10.3389/fmars.2019.00243

62. White DC, Jack R.F., Dowling N.J.E., Franklin M., Nivens D.E., Brooks S., Mittleman M.W., Vass A.A, Microbial influenced corrosion of carbon steels. *Corrosion90.* 1990;(1):103-103/12.

63. Wickham H (2016) ggplot2: Elegant Graphics for Data Analysis. *Springer-Verlag New York*.

64. Wickham H (2017) tidyverse: Easily install and Load the 'Tidyverse'. R package Version 1.2.1. https://CRAN.R-project.org/package=tidyverse

65. Xu D, Jia R, Li Y, Gu T. Advances in the treatment of problematic industrial biofilms. *World J Microbiol Biotechnol*. 2017;33(5). doi:10.1007/s11274-016-2203-4

66. Xu D, Gu T. Carbon source starvation triggered more aggressive corrosion against carbon steel by the Desulfovibrio vulgaris biofilm. *Int Biodeterior Biodegrad*. 2014;91:74-81. doi:10.1016/j.ibiod.2014.03.014